Heterogeneity in transmissibility and shedding SARS-CoV-2 via droplets and aerosols

Paul Z. Chen[1], Niklas Bobrovitz[2-4], Zahra Premji[5], Marion Koopmans[6], David N. Fisman[7,8], Frank X. Gu[1,9]*

[1]Department of Chemical Engineering & Applied Chemistry, University of Toronto, Toronto, Canada

[2]Temerty Faculty of Medicine, University of Toronto, Toronto, Canada

[3]Department of Critical Care Medicine, Cumming School of Medicine, University of Calgary, Calgary, Canada

[4]O'Brien Institute of Public Health, University of Calgary, Calgary, Canada

[5]Libraries & Cultural Resources, University of Calgary, Calgary, Canada

[6]Department of Viroscience, Erasmus University Medical Center, Rotterdam, Netherlands

[7]Division of Epidemiology, Dalla Lana School of Public Health, University of Toronto, Toronto, Canada

[8]Division of Infectious Diseases, Temerty Faculty of Medicine, University of Toronto, Toronto, Canada

[9]Institute of Biomedical Engineering, University of Toronto, Toronto, Canada

*Correspondence: f.gu@utoronto.ca

Abstract

A growing number of studies provide insight into how SARS-CoV-2 spreads[1-7]. Yet, many factors that characterize its transmissibility remain unclear, including mechanistic correlates of overdispersion, viral kinetics, the extent to which respiratory droplets and aerosols carry viable virus and the infectiousness of asymptomatic, presymptomatic and pediatric cases[7]. Here, we developed a comprehensive dataset of respiratory viral loads (rVLs) via systematic review and investigated these factors using meta-analyses and modeling. By comparing cases of COVID-19, SARS and influenza A(H1N1)pdm09, we found that heterogeneity in rVL was associated with overdispersion and facilitated the distinctions in individual variation in infectiousness among these emergent diseases. For COVID-19, case heterogeneity was broad throughout the infectious period, although rVL tended to peak at 1 day from symptom onset (DFSO) and be elevated for 1-5 DFSO. While most cases presented minimal risk, highly infectious ones could spread SARS-CoV-2 by talking, singing or breathing, which shed virions at comparable rates via droplets and aerosols. Coughing shed considerable quantities of virions, predominantly via droplets, and greatly increased the contagiousness of many symptomatic cases relative to asymptomatic ones. Asymptomatic and symptomatic infections showed similar likelihoods of expelling aerosols with SARS-CoV-2, as did adult and pediatric cases. Children tended to be less contagious by droplet spread than adults based on tendencies of symptomatology rather than rVL. Our findings address longstanding questions on SARS-CoV-2 transmissibility and present pertinent considerations for disease control.

41 **Main body**

42 The novel coronavirus SARS-CoV-2 has spread globally, causing the coronavirus disease 2019
43 (COVID-19) pandemic with more than 38.0 million infections and 1.0 million deaths (as of 13
44 October 2020)[8]. While the basic reproductive number has been estimated to be 2-3.6[1,2],
45 transmissibility of SARS-CoV-2 is highly overdispersed, with numerous instances of
46 superspreading[9-11] and few cases (10-20%) causing many secondary infections (80%)[4-6].
47 Estimates indicate 40-87% of cases are asymptomatic or paucisymptomatic, which facilitates
48 transmission[2,3,12]. Infectiousness begins around -3 to -2 DFSO and has been estimated to last 8-
49 10 DFSO[13-15]. Hence, the temporal infectiousness profile of COVID-19 resembles that of
50 influenza[16], whereas its overdispersion is similar to that of severe acute respiratory syndrome
51 (SARS)[17].

52 For respiratory virus transmission, airway epithelial cells shed virions to the extracellular
53 fluid before atomization (from breathing, talking, singing, coughing and aerosol-generating
54 procedures) partitions them into a polydisperse mixture of droplets (>5 μm) and aerosols (≤5
55 μm) that are expelled to the ambient environment[7]. Based on mass, droplets tend to settle
56 gravitationally, whereas aerosols remain suspended and travel based on airflow profiles.
57 Although proximity has been associated with infection risk for COVID-19[18], studies have also
58 suggested that long-range aerosol spread occurs conditionally[9-11].

59 Despite these analyses, key factors that characterize the transmissibility of SARS-CoV-2
60 remain unclear. To investigate many of these factors, we synthesized evidence by systematic
61 review, compared SARS-CoV-2 rVLs among subgroups, associated overdispersion, analyzed
62 viral kinetics and modeled the likelihood of shedding viable virus via droplets and aerosols
63 across respiratory activities, DFSO, case heterogeneity and subgroups. For inference on

transmissibility, we compared these analyses with those of SARS-CoV-1 (the most closely related human coronavirus) and A(H1N1)pdm09 (the most recent pandemic influenza virus), which spread by contact, droplets and aerosols[19,20].

Systematic review

To develop the comprehensive dataset, we conducted a systematic review on quantitative VL measurements for respiratory specimens taken during the infectious periods of SARS-CoV-2 (-3 to 10 DFSO)[13-15], SARS-CoV-1 (0-20 DFSO)[21] and A(H1N1)pdm09 (-2 to 9 DFSO)[16] (Methods). The systematic search (Supplementary Tables 1-5) identified 4,274 results. After screening and full-text review, 63 studies met the inclusion criteria and were used for analysis (Fig. 1) (n=9,692 total specimens), which included adult (n=5,124) and pediatric (n=1,593) cases and measurements for asymptomatic (n=2,378), presymptomatic (n=28) and symptomatic (n=7,231) infections. According to a hybrid Joanna Briggs Institute critical appraisal checklist, risk of bias was low to moderate for included studies (Extended Data Table 1).

Meta-analysis and subgroup analyses of rVL

For each study in the systematic dataset, we used specimen concentrations to estimate rVLs (Methods). We then performed a random-effects meta-analysis (Extended Data Fig. 1), which showed that, during the infectious periods, the expected rVL of SARS-CoV-2 was comparable to that of SARS-CoV-1 (p=0.148, two-sided Welch's t-test) but lesser than that of A(H1N1)pdm09 (p<0.0001). We also performed random-effects subgroup analyses for COVID-19 (Fig. 2), which showed that expected SARS-CoV-2 rVLs were consistent between pediatric and adult cases (p=0.861) and between symptomatic/presymptomatic and asymptomatic infections (p=0.951).

87

88 **Association of heterogeneity in rVL with overdispersion**

89 Since few cases drive the transmission of SARS-CoV-2 (dispersion parameter *k*, 0.10-0.58)[4-6]
90 and SARS-CoV-1 (*k*, 0.16-0.17)[17] whereas A(H1N1)pdm09 (*k*, 7.4-14.4)[22,23] spreads more
91 homogeneously, we sought to find a mechanistic association for overdispersion. As an empirical
92 estimate, *k* depends on myriad extrinsic (behavioral, environmental and invention) and host (host
93 defenses) factors. However, since dispersion is similar across distinct outbreaks of a virus[17], we
94 hypothesized that an intrinsic virological factor mediates *k* for these emergent respiratory
95 infections.

96 We assessed heterogeneity in rVL. For all three viruses, rVLs best conformed to Weibull
97 distributions (Extended Data Fig. 2), and we fitted the entirety of individual sample data for each
98 virus in the systematic dataset (Fig. 3a, Extended Data Fig. 2n). While COVID-19 and SARS
99 cases tended to shed lesser virus than those with A(H1N1)pdm09 (Extended Data Fig. 1), broad
100 heterogeneity in rVL inverted this relationship for highly infectious individuals (Extended Data
101 Fig. 3a-c). At the 90th case percentile (cp), the estimated rVL was 8.91 (8.82-9.00, 95%
102 confidence interval [CI]) $\log_{10}$ copies/ml for SARS-CoV-2, whereas it was 8.62 (8.47-8.76) $\log_{10}$
103 copies/ml for A(H1N1)pdm09. Moreover, heterogeneity in rVL was similar among adult,
104 pediatric, symptomatic/presymptomatic and asymptomatic COVID-19 cases (Extended Data Fig.
105 3d-g), with standard deviations (SDs) of 2.01-2.06 $\log_{10}$ copies/ml (Extended Data Table 2).

106 To investigate the relationship between *k* and heterogeneity in rVL, we performed a meta-
107 regression using each included study (Fig. 3b). The analysis showed a negative association
108 (p=0.031, meta-regression slope *t*-test), indicating that heterogeneity in rVL intrinsically
109 facilitated the distinctions in overdispersion among the emergent infections.

110

111 **Kinetics of SARS-CoV-2 rVL**

112 To investigate dynamics, we delineated SARS-CoV-2 rVLs by DFSO and fitted the mean
113 estimates to a mechanistic epithelial cell-limited model for viral kinetics (Fig. 3c, Methods). The
114 outputs indicated that, on average, each productively infected cell in the airway epithelium shed
115 SARS-CoV-2 at 1.11 (0.51-1.71, 95% CI) copies/ml day^{-1} and infected up to 10.6 susceptible
116 cells (Extended Data Table 3). The turnover rate for infected epithelial cells was 0.55 (0.23-0.87)
117 $days^{-1}$, while the half-life of SARS-CoV-2 in the respiratory tract was 4.35 (2.23-97.8) hours. By
118 extrapolating the model to an initial rVL of 0-1 log_{10} copies/ml, the estimated incubation period
119 was 5.38-4.52 days, which agrees with epidemiological findings[1]. Conversely, the expected
120 duration of shedding was 26.8 DFSO. Thus, SARS-CoV-2 replicated exponentially in the
121 respiratory tract based on a mean rate constant of 4.02×10^{-7} (3.01×10^{-7}-5.03×10^{-7}) $(copies/ml)^{-1}$
122 day^{-1} after infection. Around 1 DFSO, rVL peaked, as the number of infected epithelial cells
123 reached equilibrium, and then diminished exponentially.

124 As SARS-CoV-2 rVLs showed widespread heterogeneity across the infectious period, we
125 fitted distributions for each DFSO (Fig. 3d), which showed that high rVLs also increased from
126 the presymptomatic period before decreasing towards the end of the first week of illness. At the
127 90th cp, SARS-CoV-2 rVL peaked at 1 DFSO at 9.83 (9.12-10.61) log_{10} copies/ml, an order of
128 magnitude greater than the overall 90th-cp estimate (Extended Data Table 2). The estimate
129 remained ≥9.33 log_{10} copies/ml between 1-5 DFSO. At -1 DFSO, the 90th-cp rVL was 8.30
130 (6.88-10.02) log_{10} copies/ml, while it was 7.92 (7.34-8.55) log_{10} copies/ml at 10 DFSO
131 (Extended Data Fig. 3h-s).

132

133 **Likelihood of droplets and aerosols containing virions**

134 Since rVL is an intensive quantity, the volume fraction of virions is low and viral partitioning
135 coincides with atomization, we used Poisson statistics to model likelihood profiles. To calculate
136 an unbiased estimator of partitioning (the expected number of viable copies per particle), our
137 method multiplied rVL estimates with the volumes of atomized particles and an assumed
138 viability proportion of 0.1% after dehydration (Methods).

139 When expelled by the mean COVID-19 case across the infectious period, respiratory
140 particles showed minimal likelihoods of carrying viable SARS-CoV-2 (Fig. 4a,b). Aerosols
141 (dehydrated aerodynamic diameter [d_a]≤5 μm) were <0.001% likely to contain a virion. Droplets
142 also had low likelihoods: at d_a=40 μm, they were ≤0.4% likely to contain a virion.

143 COVID-19 cases with high rVLs, however, expelled particles with considerably greater
144 likelihoods of carrying viable copies (Fig. 4a,b). For the 98th cp at 1 DFSO, 18.2% (8.8-27.6%)
145 of aerosols (d_a=5 μm) contained at least one SARS-CoV-2 virion. For d_a>14.4 μm, droplets were
146 >99% likely to contain virions, with large ones carrying tens to hundreds.

147

148 **Shedding SARS-CoV-2 via respiratory activities**

149 Using the partitioning estimates in conjunction with published profiles of the particles expelled
150 by respiratory activities (Extended Data Fig. 4), we modeled the rates at which talking, singing,
151 breathing and coughing shed viable SARS-CoV-2 across d_a (Fig. 4c-f). Among the non-
152 presenting activities, singing emitted virions most rapidly followed by talking and then
153 breathing, although talking loudly was similar to singing (Extended Data Fig. 4c,d). These
154 activities produced more aerosols than droplets, but particle size correlated with the likelihood of
155 containing virions. Thus, talking, singing and breathing shed SARS-CoV-2 at similar rates via

156 aerosols and droplets: aerosols mediated 25.2-43.4% of the virions expelled by the non-
157 presenting activities (Fig. 4g). In comparison, coughing shed far greater quantities of virions
158 (Fig. 4f), of which >99.9% were carried by droplets.

159 We further examined the influences of case heterogeneity and disease course on expelling
160 SARS-CoV-2 (Fig. 4h, Extended Data Fig. 5). The estimated total shedding rates (over all
161 particle sizes) for a respiratory activity spanned ≥8.55 orders of magnitude on each DFSO;
162 cumulatively from -1 to 10 DFSO, they spanned 11.2 orders of magnitude. Hence, most cases
163 expelled a negligible number of SARS-CoV-2 virions by talking, singing or breathing. Shedding
164 occurred most rapidly at 1 DFSO: for the 98th cp, singing discharged 31.5 (3.26-379, 95% CI)
165 virions/min to the ambient environment, while talking emitted 4.67 (0.48-56.1) virions/min and
166 breathing exhaled 1.27 (0.13-15.2) virions/min; these estimates were two orders of magnitude
167 greater than those for the 86th cp. For the 98th cp at -1 DFSO, singing shed 1.31 (0.01-406)
168 virions/min and breathing exhaled 5.24×10^{-2} (5.28×10^{-4}-16.3) virions/min. The estimates at 7-10
169 DFSO were comparable to these presymptomatic ones (Fig. 4h, Extended Data Fig. 5).

170 At 1 DFSO, coughing expelled 2.13×10^{6} (2.20×10^{5}-2.56×10^{7}) virions/cough for the 98th cp,
171 90.4 (24.6-372) virions/cough for the 50th cp and 2.66 (0.65-13.1) virions/cough for the 25th cp
172 (Extended Data Fig. 5c). At -1 and 10 DFSO, these estimates were reduced by ~2 orders of
173 magnitude. Thus, most symptomatic cases shed considerable quantities of SARS-CoV-2 by
174 coughing; a single cough accounted for the virions emitted by weeks of singing for a case.

175 As indicated by similar mean rVLs (Fig. 2) and heterogeneities in rVL (Extended Data
176 Table 2), asymptomatic, symptomatic/presymptomatic, adult and pediatric COVID-19 cases
177 showed similar profiles for total shedding rates (Extended Fig. 6a-d). The estimates showed that
178 the top 6.1%, 2.4% and 1.1% of pediatric cases shed ≥1 virion/min by singing, talking and

179 breathing, respectively, while 62.5% expelled ≥10 virions/cough. In general, highly infectious
180 COVID-19 cases expelled virions more rapidly than did ones with A(H1N1)pdm09 (Extended
181 Data Fig. 6f).
182
183 **Discussion**
184 This study provided comprehensive, systematic analyses of several factors characterizing the
185 transmissibility of SARS-CoV-2. First, we evaluated the influence of heterogeneity in rVL. Our
186 findings show that broad heterogeneity in rVL facilitates greater variation in individual
187 infectiousness in the COVID-19 pandemic than was found in the 2009 H1N1 pandemic. For each
188 respiratory activity, SARS-CoV-2 shedding rates span >11 orders of magnitude throughout the
189 infectious period. While most COVID-19 cases present minimal transmission risk by talking,
190 singing or breathing, highly infectious ones, including asymptomatic and presymptomatic
191 infections, can spread SARS-CoV-2 through these activities. Our model estimates, when
192 corrected to copies rather than virions, align with recent clinical findings for exhalation rates of
193 SARS-CoV-2[24]. Moreover, the findings suggest that heterogeneity in rVL may be a virological
194 factor generally associated with overdispersion for respiratory infections. In this case, rVL
195 distribution may serve as an early correlate for transmission patterns, including superspreading,
196 during outbreaks of novel respiratory viruses, providing insight for disease control before large-
197 scale epidemiological analyses empirically characterize *k*.
198 Second, we analyzed SARS-CoV-2 kinetics during respiratory infection. While
199 heterogeneity remains broad throughout the infectious period, the systematic dataset indicates
200 that rVL tends to peak at 1 DFSO and be elevated for 1-5 DFSO, coinciding with the period of
201 highest attack rates observed among close contacts[25]. These results indicate that transmission risk

202 tends to be greatest soon after illness rather than in the presymptomatic period, which concurs
203 with large tracing studies (6.4-12.6% of secondary infections from presymptomatic
204 transmission)[26,27] rather than early temporal models (~44%)[14]. Furthermore, our kinetic analysis
205 suggests that, on average, SARS-CoV-2 reaches diagnostic concentrations 1.60-3.22 days after
206 respiratory infection (-3.78 to -2.16 DFSO), assuming assay detection limits of 1-3 $\log_{10}$
207 copies/ml, respectively, for nasopharyngeal swabs immersed in 1 ml of transport media.
208 Third, we modeled the likelihood of shedding SARS-CoV-2 via aerosols. Talking, singing
209 and breathing shed SARS-CoV-2 at comparable rates through droplets and aerosols (up to tens to
210 hundreds of virions/min). As airborne spread is recognized as a key mode of transmission for
211 A(H1N1)pdm09[20], our model estimates and comparative analyses support, particularly for highly
212 infectious cases, airborne spread as a transmission mode for SARS-CoV-2. While our models
213 delineated aerosols from droplets at the classical threshold (d_a=5 μm), recent reports show that,
214 based on emission vectors and environmental conditions, respiratory particles larger than 5 μm
215 can also travel >2 m in air[28,29], further supporting the plausibility of the airborne transmission of
216 SARS-CoV-2. However, with short durations of stay in well-ventilated areas, the concentration,
217 and exposure risk, of aerosols remains correlated with proximity to infectious cases[18,28].
218 Fourth, we assessed the relative infectiousness of COVID-19 subgroups. Since rVL
219 distributions are similar among subgroups and the predominant source of aerosols is the non-
220 presenting respiratory activities (talking, singing and breathing), symptomatic and asymptomatic
221 infections present similar risks for aerosol spread, as do adult and pediatric cases. However, most
222 cases shed considerable numbers of virions via large droplets by coughing, a common symptom
223 of COVID-19[30]. Thus, symptomatic infections tend to be significantly more contagious than
224 asymptomatic ones, providing a reason as to why asymptomatic cases transmit SARS-CoV-2 at

225 lower relative rates[3], especially in close contact[31], despite similar rVLs and increased contact
226 patterns. Accordingly, children (48-54% of symptomatic cases present with cough)[32,33] tend to be
227 less contagious by droplet spread than adults (68-80%)[30,33] based on tendencies of
228 symptomatology rather than rVL.

229 Our study has limitations. The systematic search found a limited number of studies reporting
230 quantitative specimen measurements from the presymptomatic period, meaning these estimates
231 may be sensitive to sampling bias. Although additional studies have reported semiquantitative
232 metrics (cycle thresholds), these data were excluded because they cannot be compared on an
233 absolute scale due to batch effects[34], limiting use in compound analyses. Furthermore, our
234 analyses considered population-level estimates of the infectious periods and viability
235 proportions, which omit individual variation in the dynamics of virus viability. Some patients
236 shed SARS-CoV-2 with diminishing viability soon after symptom onset[13], while others produce
237 replication-competent virus for weeks[35]. It remains unelucidated how case characteristics and
238 environmental factors affect the viability dynamics of SARS-CoV-2.

239 Taken together, our findings provide a potential path forward for disease control. They
240 highlight the disproportionate role of high-risk cases, settings and circumstances in propelling
241 the COVID-19 pandemic. Since highly infectious cases, regardless of age or symptomatology,
242 can rapidly shed SARS-CoV-2 via both droplets and aerosols, airborne spread should also be
243 recognized as a transmission risk, including for superspreading. Strategies to abate infection
244 should limit crowd numbers and duration of stay while reinforcing distancing and then
245 widespread mask usage; well-ventilated settings can be recognized as lower risk venues.
246 Coughing sheds considerable quantities of virions for most infections, while rVL tends to peak at
247 1 DFSO and can be high throughout the infectious period. Thus, immediate, sustained self-

248 isolation upon symptom presentation is crucial to curb transmission from symptomatic cases.
249 While diagnosing COVID-19, qRT-PCR can also help to triage contact tracing, prioritizing
250 patients with higher specimen measurements: for nasopharyngeal swabs immersed in 1 ml of
251 transport media, ≥7.14 (7.07-7.22, 95% CI) $\log_{10}$ copies/ml corresponds to ≥80th cp. Doing so
252 may identify asymptomatic and presymptomatic cases more efficiently, a key step towards
253 mitigation as the pandemic continues.

254 **References**

255 1 Li, Q. *et al.* Early transmission dynamics in Wuhan, China, of novel coronavirus-infected
256 pneumonia. *N. Engl. J. Med.* **382**, 1199-1207, doi:10.1056/NEJMoa2001316 (2020).
257 2 Hao, X. *et al.* Reconstruction of the full transmission dynamics of COVID-19 in Wuhan.
258 *Nature* **584**, 420-424, doi:10.1038/s41586-020-2554-8 (2020).
259 3 Li, R. *et al.* Substantial undocumented infection facilitates the rapid dissemination of novel
260 coronavirus (SARS-CoV-2). *Science* **368**, 489-493, doi:10.1126/science.abb3221 (2020).
261 4 Endo, A., Abbott, S., Kucharski, A. J. & Funk, S. Estimating the overdispersion in
262 COVID-19 transmission using outbreak sizes outside China. *Wellcome Open Research* **5**,
263 doi:10.12688/wellcomeopenres.15842.1 (2020).
264 5 Laxminarayan, R. *et al.* Epidemiology and transmission dynamics of COVID-19 in two
265 Indian states. *Science*, eabd7672, doi:10.1126/science.abd7672 (2020).
266 6 Bi, Q. *et al.* Epidemiology and transmission of COVID-19 in 391 cases and 1286 of their
267 close contacts in Shenzhen, China: a retrospective cohort study. *Lancet Infect. Dis.* **20**,
268 911-919, doi:10.1016/s1473-3099(20)30287-5 (2020).
269 7 Organization, W. H. Transmission of SARS-CoV-2: implications for infection prevention
270 precautions (scientific brief). July 9, 2020.
271 8 Dong, E., Du, H. & Gardner, L. An interactive web-based dashboard to track COVID-19 in
272 real time. *Lancet Infect. Dis.* **20**, 533-534, doi:10.1016/S1473-3099(20)30120-1 (2020).
273 9 Shen, Y. *et al.* Community outbreak investigation of SARS-CoV-2 transmission among
274 bus riders in Eastern China. *JAMA Intern. Med.*, doi:10.1001/jamainternmed.2020.5225
275 (2020).

276 10 Lu, J. *et al.* COVID-19 outbreak associated with air conditioning in restaurant, Guangzhou,
277 China, 2020. *Emerg. Infect. Dis.* **26**, 1628-1631, doi:10.3201/eid2607.200764 (2020).
278 11 Hamner, L. *et al.* High SARS-CoV-2 attack rate following exposure at a choir practice -
279 Skagit County, Washington, March 2020. *MMWR Morb. Mortal. Wkly. Rep.* **69**, 606-610,
280 doi:10.15585/mmwr.mm6919e6 (2020).
281 12 Oran, D. P. & Topol, E. J. Prevalence of asymptomatic SARS-CoV-2 infection: a narrative
282 review. *Ann. Intern. Med.* **173**, 362-367, doi:10.7326/M20-3012 (2020).
283 13 Wolfel, R. *et al.* Virological assessment of hospitalized patients with COVID-2019. *Nature*
284 **581**, 465-469, doi:10.1038/s41586-020-2196-x (2020).
285 14 He, X. *et al.* Temporal dynamics in viral shedding and transmissibility of COVID-19. *Nat.*
286 *Med.* **26**, 672-675, doi:10.1038/s41591-020-0869-5 (2020).
287 15 Arons, M. M. *et al.* Presymptomatic SARS-CoV-2 infections and transmission in a skilled
288 nursing facility. *N. Engl. J. Med.* **382**, 2081-2090, doi:10.1056/NEJMoa2008457 (2020).
289 16 Ip, D. K. *et al.* Viral shedding and transmission potential of asymptomatic and
290 paucisymptomatic influenza virus infections in the community. *Clin. Infect. Dis.* **64**, 736-
291 742, doi:10.1093/cid/ciw841 (2017).
292 17 Lloyd-Smith, J. O., Schreiber, S. J., Kopp, P. E. & Getz, W. M. Superspreading and the
293 effect of individual variation on disease emergence. *Nature* **438**, 355-359,
294 doi:10.1038/nature04153 (2005).
295 18 Chu, D. K. *et al.* Physical distancing, face masks, and eye protection to prevent person-to-
296 person transmission of SARS-CoV-2 and COVID-19: a systematic review and meta-
297 analysis. *Lancet* **395**, 1973-1987, doi:10.1016/S0140-6736(20)31142-9 (2020).

298 19 Yu, I. T. *et al.* Evidence of airborne transmission of the severe acute respiratory syndrome
299 virus. *N. Engl. J. Med.* **350**, 1731-1739, doi:10.1056/NEJMoa032867 (2004).
300 20 Cowling, B. J. *et al.* Aerosol transmission is an important mode of influenza A virus
301 spread. *Nat. Commun.* **4**, 1935, doi:10.1038/ncomms2922 (2013).
302 21 Pitzer, V. E., Leung, G. M. & Lipsitch, M. Estimating variability in the transmission of
303 severe acute respiratory syndrome to household contacts in Hong Kong, China. *Am. J.*
304 *Epidemiol.* **166**, 355-363, doi:10.1093/aje/kwm082 (2007).
305 22 Roberts, M. G. & Nishiura, H. Early estimation of the reproduction number in the presence
306 of imported cases: pandemic influenza H1N1-2009 in New Zealand. *PLoS One* **6**, e17835,
307 doi:10.1371/journal.pone.0017835 (2011).
308 23 Brugger, J. & Althaus, C. L. Transmission of and susceptibility to seasonal influenza in
309 Switzerland from 2003 to 2015. *Epidemics* **30**, 100373, doi:10.1016/j.epidem.2019.100373
310 (2020).
311 24 Ma, J. *et al.* COVID-19 patients in earlier stages exhaled millions of SARS-CoV-2 per
312 hour. *Clin. Infect. Dis.*, doi:10.1093/cid/ciaa1283 (2020).
313 25 Cheng, H. Y. *et al.* Contact tracing assessment of COVID-19 transmission dynamics in
314 Taiwan and risk at different exposure periods before and after symptom onset. *JAMA*
315 *Intern. Med.*, doi:10.1001/jamainternmed.2020.2020 (2020).
316 26 Wei, W. E. *et al.* Presymptomatic transmission of SARS-CoV-2 — Singapore, January 23-
317 March 16, 2020. *MMWR Morb. Mortal. Wkly. Rep.* **69**, 411-415,
318 doi:10.15585/mmwr.mm6914e1 (2020).
319 27 Du, Z. *et al.* Serial interval of COVID-19 among publicly reported confirmed cases.
320 *Emerg. Infect. Dis.* **26**, 1341-1343, doi:10.3201/eid2606.200357 (2020).

321 28 Abkarian, M., Mendez, S., Xue, N., Yang, F. & Stone, H. A. Speech can produce jet-like
322 transport relevant to asymptomatic spreading of virus. *Proc. Natl. Acad. Sci. U. S. A.*,
323 doi:10.1073/pnas.2012156117 (2020).
324 29 Bourouiba, L. Turbulent gas clouds and respiratory pathogen emissions: potential
325 implications for reducing transmission of COVID-19. *JAMA* **323**, 1837-1838,
326 doi:10.1001/jama.2020.4756 (2020).
327 30 Guan, W. J. *et al.* Clinical characteristics of coronavirus disease 2019 in China. *N. Engl. J.*
328 *Med.* **382**, 1708-1720, doi:10.1056/NEJMoa2002032 (2020).
329 31 Luo, L. *et al.* Contact settings and risk for transmission in 3410 close contacts of patients
330 with COVID-19 in Guangzhou, China: a prospective cohort study. *Ann. Intern. Med.*,
331 doi:10.7326/M20-2671 (2020).
332 32 Lu, X. *et al.* SARS-CoV-2 infection in children. *N. Engl. J. Med.* **382**, 1663-1665,
333 doi:10.1056/NEJMc2005073 (2020).
334 33 CDC COVID-19 Response Team. Coronavirus disease 2019 in children - United States,
335 February 12-April 2, 2020. *MMWR Morb. Mortal. Wkly. Rep.* **69**, 422-426,
336 doi:10.15585/mmwr.mm6914e4 (2020).
337 34 Han, M. S., Byun, J. H., Cho, Y. & Rim, J. H. RT-PCR for SARS-CoV-2: quantitative
338 versus qualitative. *Lancet Infect. Dis.*, doi:10.1016/S1473-3099(20)30424-2 (2020).
339 35 van Kampen, J. J. A. *et al.* Shedding of infectious virus in hospitalized patients with
340 coronavirus disease-2019 (COVID-19): duration and key determinants. Preprint at
341 medRxiv doi:10.1101/2020.06.08.20125310 (2020).

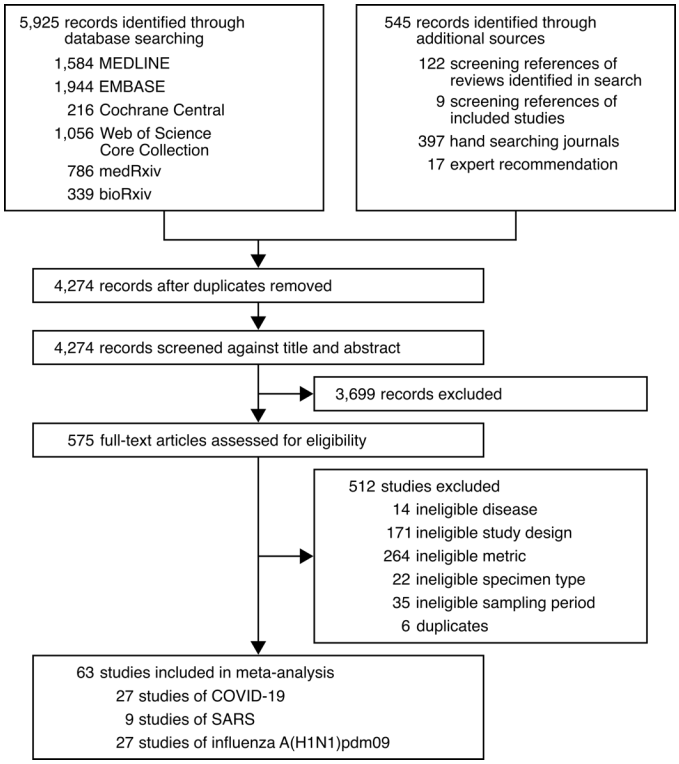

Fig. 1. Development of the systematic dataset.

Subgroup, study ref.	Cases No.	Cases Type	Specimens No.	Specimens DFSO	Specimens Type	Respiratory viral load, $\log_{10}$ copies/ml (95% CI)	*p*-value for difference
Adult							
42	4	H, A, S	9	4 to 10	NPS, OPS	4.12 (3.18-5.05)	
43	100	H, C, A, S, Ps, As	106	-2 to 10	NPS, OPS	4.65 (4.35-4.95)	
44	6	H, A, S	6	3 to 8	OPS	5.13 (4.83-5.42)	
45	23	H, A, S	51	0 to 10	ETA, POS	5.29 (4.65-5.93)	
46	14	H, A, S, As	55	0 to 10	NPS, OPS	5.30 (4.87-5.74)	
47	-	H, N, A, S	31	2 to 10	NPS, OPS, Spu	5.41 (4.81-6.01)	
48	-	H, A, S	19	1 to 10	POS, Spu	5.62 (5.22-6.03)	
49	2,182	C, A, As	2,182	0	NPS	6.01 (5.93-6.09)	
50	171	N, A, S	171	0 to 10	NPS	6.07 (5.79-6.34)	
51	103	H, N, A, S	103	0 to 8	NPS, OPS	6.10 (5.98-6.23)	
13	9	H, A, S, As	133	2 to 10	NPS, OPS, Spu	6.21 (5.90-6.52)	
52	41	H, A, S	310	2 to 10	NPS, OPS, POS	6.28 (6.05-6.50)	
53	5	H, A, S	5	7 to 9	NPS	6.48 (5.26-7.70)	
54	-	H, A, S, As	38	0 to 9	NPA, NPS, OPS, Spu	6.52 (5.77-7.27)	
55	347	H, A, S	347	0 to 5	NPS	6.97 (6.77-7.18)	
56	24	H, A, S	33	0 to 10	NPS	7.51 (6.97-8.05)	
57	205	H, N, A, S	205	0 to 10	NPS	7.55 (7.30-7.81)	
35	-	H, A, S	154	0 to 10	NPS, Spu	7.83 (7.58-8.08)	
58	148	N, A, S	296	1 to 8	NPS	8.04 (7.81-8.28)	
59	5	H, A, S	63	0 to 10	NPS, OPS	8.34 (7.95-8.73)	
Overall (Q_{19} = 10.1, p = 0.95, I^2 = 0.0%)						6.10 (5.96-6.24)	-
Pediatric							
43	2	H, C, P, S	3	8 to 9	NPS, OPS	3.77 (1.74-5.81)	
60	7	H, P, S, Ps, As	14	-1 to 10	NPS	5.69 (5.26-6.12)	
61	54	C, P, S, Ps, As	54	-3 to 10	NPS	5.82 (5.36-6.29)	
55	58	H, P, S	58	0 to 5	NPS	6.97 (6.45-7.49)	
62	23	H, P, S	23	0 to 4	NPS	7.20 (6.23-8.16)	
63	12	H, P, S, As	27	0 to 10	NPS	8.07 (7.47-8.67)	
Overall (Q_5 = 3.76, p = 0.59, I^2 = 0.0%)						6.15 (5.60-6.70)	0.861
Symptomatic/presymptomatic							
42	4	H, A, S	9	4 to 10	NPS, OPS	4.12 (3.18-5.05)	
43	53	H, C, A, P, S, Ps	60	-2 to 10	NPS, OPS	4.43 (4.03-4.84)	
44	6	H, A, S	6	3 to 8	OPS	5.13 (4.83-5.42)	
46	13	H, A, S	51	0 to 10	NPS, OPS	5.25 (4.79-5.71)	
45	23	H, A, S	51	0 to 10	ETA, POS	5.29 (4.65-5.93)	
47	-	H, N, A, S	31	2 to 10	NPS, OPS, Spu	5.41 (4.81-6.01)	
48	-	H, A, S	19	1 to 10	POS, Spu	5.62 (5.22-6.03)	
60	6	H, P, S, Ps	13	-1 to 10	NPS	5.77 (5.10-6.53)	
61	81	C, A, P, S, Ps	81	-3 to 10	NPS	5.78 (5.41-6.15)	
13	8	H, A, S	129	2 to 10	NPS, OPS, Spu	5.88 (5.60-6.17)	
64	75	H, S, Ps	104	-1 to 8	OPS, Spu	5.98 (5.31-6.66)	
50	171	N, A, S	171	0 to 10	NPS	6.07 (5.79-6.34)	
51	103	H, N, A, S	103	0 to 8	NPS, OPS	6.10 (5.98-6.23)	
52	41	H, A, S	310	2 to 10	NPS, OPS, POS	6.28 (6.05-6.50)	
53	5	H, A, S	5	7 to 9	NPS	6.48 (5.26-7.70)	
55	405	H, A, P, S	405	0 to 5	NPS	6.95 (6.78-7.17)	
62	23	H, P, S	23	0 to 4	NPS	7.20 (6.23-8.16)	
56	24	H, A, S	33	0 to 10	NPS	7.51 (6.97-8.05)	
57	205	H, N, A, S	205	0 to 10	NPS	7.55 (7.30-7.81)	
35	-	H, A, S	154	0 to 10	NPS, Spu	7.83 (7.58-8.08)	
65	2	H, A, P, S	8	4 to 10	NPS, OPS	7.91 (6.69-9.12)	
58	148	N, A, S	296	1 to 8	NPS	8.04 (7.81-8.28)	
63	9	H, P, S	20	0 to 10	NPS	8.10 (7.37-8.33)	
59	5	H, A, S	63	0 to 10	NPS, OPS	8.34 (7.95-8.73)	
Overall (Q_{23} = 13.2, p = 0.95, I^2 = 0.0%)						6.18 (6.06-6.29)	-
Asymptomatic							
43	49	H, C, A, As	49	0	NPS, OPS	4.89 (4.46-5.33)	
61	52	C, A, P, As	52	0	NPS	5.31 (4.85-5.77)	
49	2,200	C, A, P, As	2,200	0	NPS	6.01 (5.93-6.09)	
63	3	H, P, As	7	0 to 8	NPS	8.01 (6.91-9.11)	
Overall (Q_3 = 2.49, p = 0.48, I^2 = 0.0%)						6.15 (5.34-6.96)	0.951

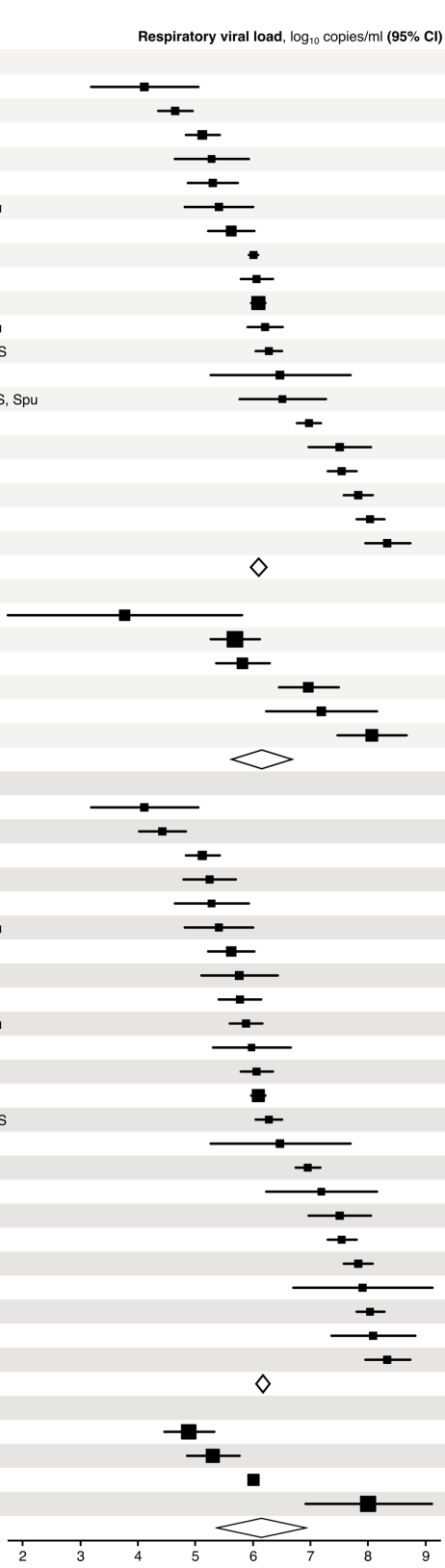

345 **Fig. 2. Subgroup analyses of SARS-CoV-2 respiratory viral load during the infectious**
346 **period.** Random-effects meta-analyses comparing the expected rVLs of adult (>18 years old)
347 COVID-19 cases with pediatric (≤18 years old) ones (top) and symptomatic/presymptomatic
348 infections with asymptomatic ones (bottom) during the infectious period. Quantitative specimen
349 measurements were used to estimate rVLs, which refer to virus concentrations in the respiratory
350 tract. Case types: hospitalized (H), not admitted (N), community (C), adult (A), pediatric (P),
351 symptomatic (S), presymptomatic (Ps) and asymptomatic (As). Specimen types: endotracheal
352 aspirate (ETA), nasopharyngeal aspirate (NPA), nasopharyngeal swab (NPS), oropharyngeal
353 swab (OPS), posterior oropharyngeal saliva (POS) and sputum (Spu). Studies after ref. 35 are
354 listed in Methods. Dashes denote case numbers that were not obtained. Box sizes are
355 proportional to weighting in the overall estimates. Two-sided Welch's *t*-tests, non-significance
356 (p>0.05).

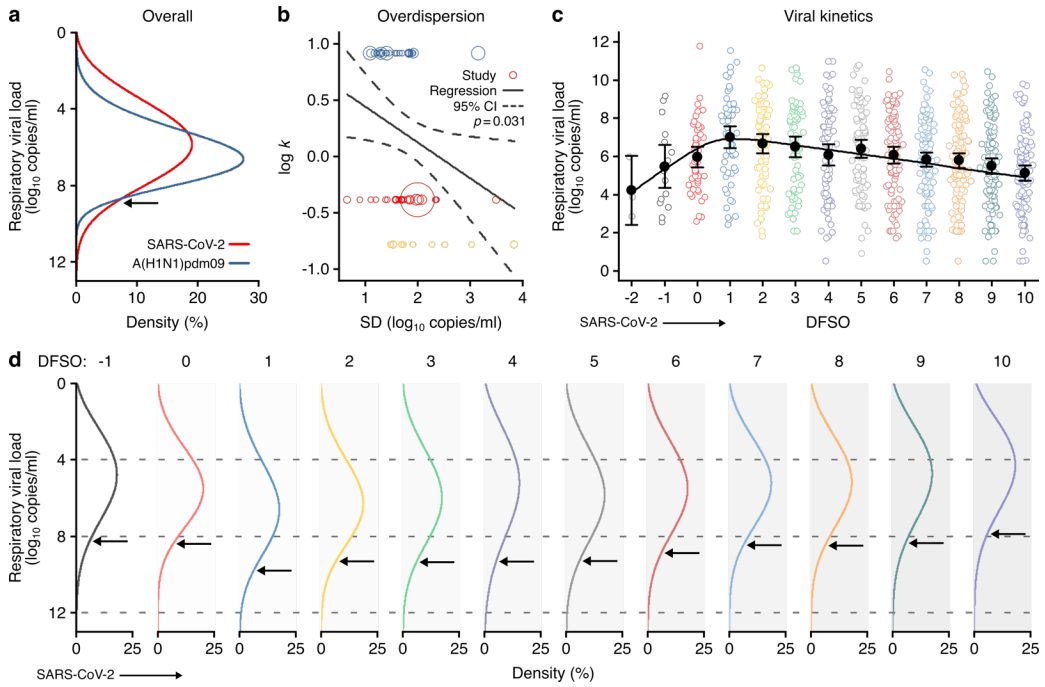

Fig. 3. Heterogeneity and kinetics of SARS-CoV-2 respiratory viral load. a, Estimated distribution of rVL for SARS-CoV-2 (n=3,778 samples from n=24 studies) and A(H1N1)pdm09 (n=512 samples from n=10 studies) throughout the infectious periods. **b,** Meta-regression of dispersion parameter (k) with the standard deviation (SD) of rVLs from included studies (r=-0.27). Estimates of k were pooled from the literature. Red, yellow and blue circles denote COVID-19 (n=27), SARS (n=9) and A(H1N1)pdm09 (n=27) studies, respectively. Circle sizes are proportional to weighting in the meta-regression. The p-value was obtained using the meta-regression slope t-test. **c,** SARS-CoV-2 rVLs fitted to a mechanistic model of viral kinetics (black curve, r^2=0.88). Filled circles and bars depict mean estimates and 95% CIs. Open circles show the entirety of individual sample data over DFSO (left to right, n=3, 15, 48, 59, 69, 71, 81, 87, 102, 125, 119, 117 and 110 samples from n=19 studies). **d,** Estimated distributions of SARS-CoV-2 rVL over DFSO. Earlier DFSO were excluded based on limited data. Weibull distributions were fitted on the entirety of individual sample data for the virus (**a**) or DFSO (**d**) in the systematic dataset. Arrows denote 90th case percentiles for SARS-CoV-2 rVL.

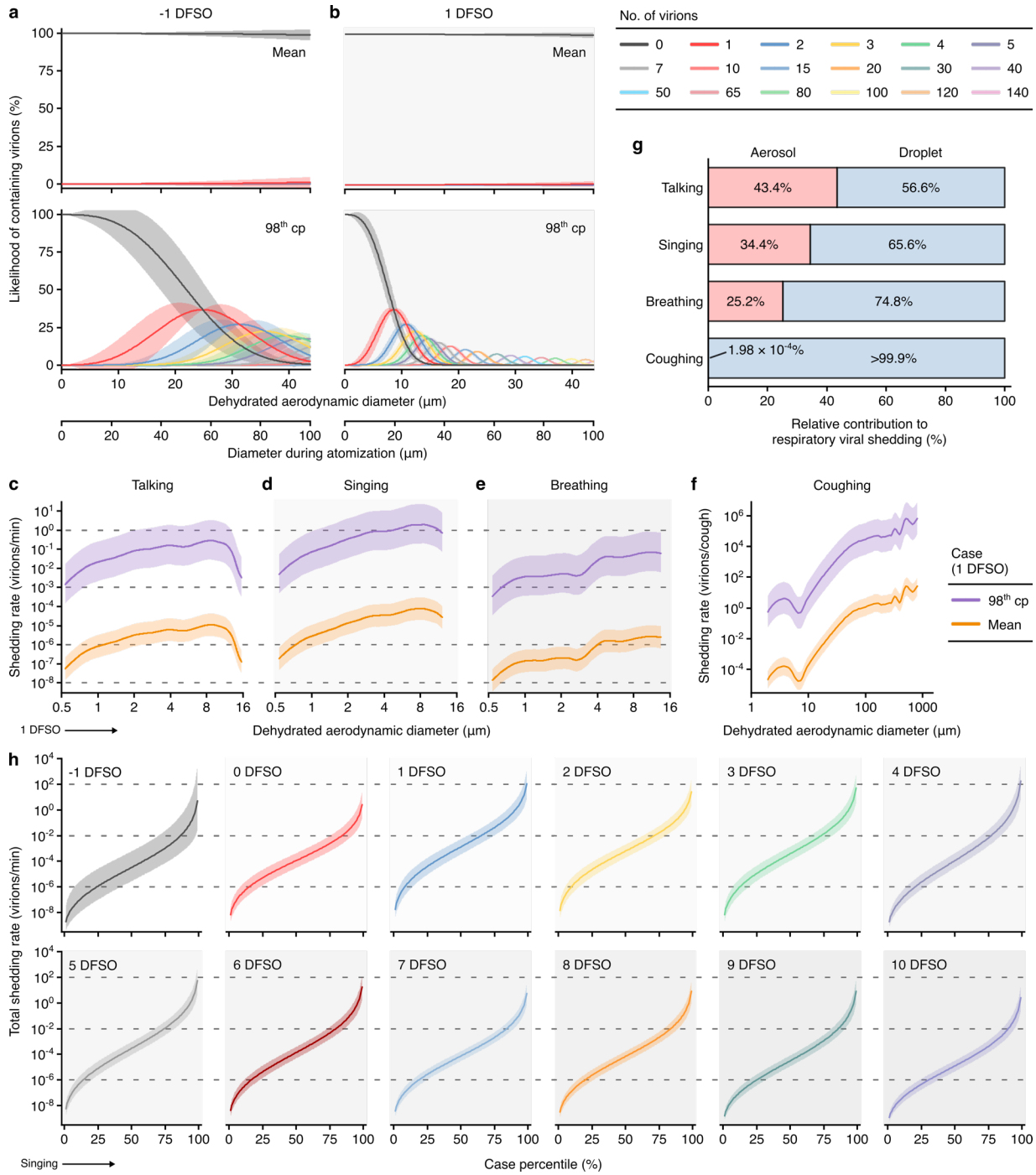

Fig. 4. Heterogeneity in shedding SARS-CoV-2 via droplets and aerosols. a,b, Likelihood of respiratory particles containing viable SARS-CoV-2 when expelled by the mean (top) or 98th case percentile (cp) (bottom) COVID-19 cases at -1 (**a**) or 1 (**b**) DFSO. The models considered virus viability within dehydrated particles. Diameters during atomization were included to show

377 their size relationship with dehydrated aerodynamic diameter (d_a), but not likelihood of
378 containing virions during atomization. For higher no. of virions, some likelihood curves were
379 omitted to aid visualization. When the likelihood for 0 virions approaches 0%, particles are
380 expected to contain at least one viable copy. **c-f**, Rate that the mean and 98th-cp COVID-19 cases
381 at 1 DFSO shed viable SARS-CoV-2 by talking (**c**), singing (**d**), breathing (**e**) or coughing (**f**)
382 over d_a. **g**, Relative contribution of aerosols ($d_a \leq 5$ μm, red bar) and droplets ($d_a > 5$ μm, blue bar)
383 to shedding virions for the respiratory activities. **h**, Case heterogeneity in the total shedding rate
384 (over all particle sizes) of virions via singing across the infectious period. Earlier
385 presymptomatic days were excluded based on limited data. Data range between the 1st and 99th
386 cps. Lines and bands represent estimates and 95% CIs, respectively, for likelihoods or Poisson
387 means.

388 **Methods**

389 **Search strategy, selection criteria and data collection**

390 We undertook a systematic review and prospectively submitted the systematic review protocol
391 for registration on PROSPERO (registration number, CRD42020204637). Other than the title of
392 this study, we have followed PRISMA reporting guidelines[36]. The systematic review was
393 conducted according to Cochrane methods guidance[37].

394 The search included papers that (i) reported positive, quantitative measurements (copies/ml
395 or an equivalent metric) of SARS-CoV-2, SARS-CoV-1 or A(H1N1)pdm09 in human
396 respiratory specimens (ETA, NPA, NPS, OPS, POS and Spu) from COVID-19, SARS or
397 A(H1N1)pdm09 cases; (ii) reported data that could be extracted from the infectious periods of
398 SARS-CoV-2 (defined as -3 to +10 DFSO for symptomatic cases and 0 to +10 days from the day
399 of laboratory diagnosis for asymptomatic cases), SARS-CoV-1 (defined as 0 to +20 DFSO or the
400 equivalent asymptomatic period) or A(H1N1)pdm09 (defined as -2 to +9 DFSO for symptomatic
401 cases and 0 days to +9 days from the day of laboratory diagnosis for asymptomatic cases); and
402 (iii) reported data for two or more cases with laboratory-confirmed COVID-19, SARS or
403 A(H1N1)pdm09. Quantitative specimen measurements were considered after RNA extraction for
404 diagnostic sequences of SARS-CoV-2 (*Ofr1b*, *N*, *RdRp* and *E* genes), SARS-CoV-1 (*Ofr1b*, *N*
405 and *RdRp* genes) and A(H1N1)pdm09 (*HA* and *M* genes).

406 Studies were excluded, in the following order, if they (i) studied an ineligible disease; (ii)
407 had an ineligible study design, including those that were reviews of evidence (e.g., scoping,
408 systematic, narrative), did not include primary clinical human data, reported data for less than
409 two cases due to an increased risk of selection bias, were incomplete (e.g., ongoing clinical
410 trials), did not report an RNA extraction step before measurement or were studies measuring

411 environmental samples; (iii) reported an ineligible metric for specimen concentration (e.g.,
412 qualitative RT-PCR or cycle threshold [Ct] values without calibration included in the study); (iv)
413 reported quantitative measurements from an ineligible specimen type (e.g., blood specimens,
414 pooled specimens or self-collected POS or Spu patient specimens in the absence of a healthcare
415 professional); (v) reported an ineligible sampling period (consisted entirely of data that could not
416 be extracted from within the infectious period); or (vi) were duplicates of an included study (e.g.,
417 preprinted version of published paper or duplicates not identified by Covidence). We included
418 data from control groups receiving standard of care in interventional studies but excluded data
419 from the intervention group. Patients in the intervention group are, by definition, systematically
420 different from general case populations because they receive therapies not being widely used for
421 treatment, which may influence virus concentrations. Interventional studies examining the
422 comparative effectiveness of two or more treatments were excluded for the same reason. Studies
423 exclusively reporting semiquantitative measurements (e.g., Ct values) of specimen concentration
424 were excluded, as these measurements are sensitive to batch inconsistencies and, without proper
425 calibration, cannot be compared on an absolute scale across studies[34].
426 We searched, without the use of filters or language restrictions, the following sources:
427 MEDLINE (via Ovid, 1946 to 7 August 2020), EMBASE (via Ovid, 1974 to 7 August 2020,
428 Cochrane Central Register of Controlled Trials (via Ovid, 1991 to 7 August 2020), Web of
429 Science Core Collection (including: Science Citation Index Expanded, 1900 to 7 August 2020;
430 Social Sciences Citation Index, 1900 to 7 August 2020; Arts & Humanities Citation Index, 1975
431 to 7 August 2020; Conference Proceedings Citation Index - Science, 1990 to 7 August 2020;
432 Conference Proceedings Citation Index - Social Sciences & Humanities, 1990 to 7 August 2020;
433 and Emerging Sources Citation Index, 2015 to 7 August 2020), as well as MedRxiv and BioRxiv

434 (both searched through Google Scholar via the Publish or Perish program, to 7 August 2020).
435 We also gathered studies by searching through the reference lists of review articles identified by
436 the database search, by searching through the reference lists of included articles, through expert
437 recommendation (by Epic J. Topol, Akiko Iwasaki and A. Marm Kilpatrick on Twitter) and by
438 hand-searching through journals (*Nature*, *Nat. Med.*, *Science*, *NEJM*, *Lancet*, *Lancet Infect. Dis.*,
439 *JAMA*, *JAMA Intern. Med.* and *BMJ*). A comprehensive search was developed by a librarian,
440 which included subject headings and keywords. The search strategy had 3 main concepts
441 (disease, specimen type and outcome), and each concept was combined using the appropriate
442 Boolean operators. The search was tested against a sample set of known articles that were pre-
443 identified. The line-by-line search strategies for all databases are included in Supplementary
444 Tables 1-5. The search results were exported from each database and uploaded to the Covidence
445 online system for deduplication and screening.

446 Two authors independently screened titles and abstracts, reviewed full texts, collected data
447 and assessed risk of bias via Covidence and a hybrid critical appraisal checklist based on the
448 Joanna Briggs Institute (JBI) tools for case series, analytical cross-sectional studies and
449 prevalence studies[38-40]. To evaluate the sample size in a study, we used the following calculation:

450 $$n^* = \frac{z^2\sigma}{d^2}, \quad (1)$$

451 where n^* is the sample size threshold, z is the z-score for the level of confidence (95%), σ is the
452 standard deviation (assumed to be 3 $\log_{10}$ copies/ml, one quarter of the full range of rVLs) and d
453 is the marginal error (assumed to be 1 $\log_{10}$ copies/ml, based on the minimum detection limit for
454 qRT-PCR across studies)[41]. The hybrid JBI critical appraisal checklist is shown in the
455 Supplementary Notes. Inconsistencies were resolved by discussion and consensus.

456 The search found 27 studies for COVID-19[13,35,42-66], 9 studies for SARS[67-75] and 27 studies
457 for A(H1N1)pdm09[76-102]. Quantitative specimen measurements were collected directly if
458 reported numerically or using WebPlotDigitizer 4.3 (https://apps.automeris.io/wpd/) if reported
459 graphically. For included studies, we also collected the relevant numbers of cases, types of cases,
460 volumes of transport media, pharmacotherapies, DFSO (for symptomatic cases) or day relative to
461 initial laboratory diagnosis (for asymptomatic cases) on which each specimen was taken and
462 numbers of tested specimens. Hospitalized cases were defined as those being tested in a hospital
463 setting and then admitted. Non-admitted cases were defined as those being testing in a hospital
464 setting but not admitted. Community cases were defined as those being tested in a community
465 setting. Symptomatic, presymptomatic and asymptomatic infections were defined as in the study.
466 Based on rare description in the included studies, paucisymptomatic infections, when defined in
467 a study, were included with symptomatic ones. Pediatric cases were defined as those of 18 years
468 of age or lower or as defined in the study. Adult cases were defined as those above 18 years of
469 age or as defined in the study.
470
471 **Meta-analysis of rVLs**
472 Based on the search design and composition of included studies, the meta-analysis overall
473 estimates were the expected SARS-CoV-2, SARS-CoV-1 and A(H1N1)pdm09 rVL when
474 encountering a COVID-19, SARS or A(H1N1)pdm09 case, respectively, during their infectious
475 period. To determine rVLs, data collected on positive, quantitative specimen measurements were
476 converted to the RNA concentration in the respiratory tract. Viral concentrations in respiratory
477 specimens were denoted as specimen measurements, whereas viral concentrations in the
478 respiratory tract were denoted as rVLs. For example, measurements from swabbed specimens

479 (NPS and OPS) typically report the RNA concentration in viral transport media. Based on the
480 expected uptake volume for swabs (0.128 ± 0.031 ml, mean ± SD)[103] or reported collection
481 volume for expulsed fluid in each study (e.g., 0.5 to 1 ml) along with the reported volume of
482 transport media in each study (e.g., 1 ml), we calculated the dilution factor for each respiratory
483 specimen to estimate the rVLs. If the diluent volume was not reported, then the dilution factor
484 was calculated assuming a volume of 1 ml (NPS and OPS), 2 ml (POS and ETA) or 3 ml (NPA)
485 of transport media[43,45,71]. Unless dilution was reported for Spu specimens, we used the specimen
486 measurement as the rVL[13]. The non-reporting of diluent volume was noted as an element
487 increasing risk of bias in the hybrid JBI critical appraisal checklist. Viral load estimates (based
488 on instrumentation, calibration, procedures and reagents) are not standardized. While the above
489 procedures (including only quantitative measurements after extraction, collecting assay detection
490 limits, correcting for specimen dilution) have considered many of these factors, non-
491 standardization is an inherent limitation in interpreting specimen measurements across studies.
492 Pooled estimates and 95% CIs for the expected rVL of each virus across their infectious
493 period were calculated using a random-effects meta-analysis. The estimates for rVL assumed
494 that each viral copy was extracted and quantified from the tested specimen aliquot. For studies
495 reporting summary statistics in medians and interquartile or total ranges, we derived estimates of
496 the mean and variance and calculated the 95% CIs[104]. All calculations were performed in units of
497 $\log_{10}$ copies/ml. Between-study heterogeneity in meta-analysis was assessed using the I^2 and τ^2
498 statistics. The weighting for each study in its virus group was calculated as the reciprocal of the
499 rVL variance.
500
501 **Subgroup analyses of rVLs**

502 Subgroup analyses were conducted to compare the expected rVLs of SARS-CoV-2 in adult,
503 pediatric, symptomatic and asymptomatic COVID-19 cases, as previously defined, during the
504 infectious period. The overall estimate for each subgroup was the expected rVL when
505 encountering a case of that subgroup during the infectious period. Studies reporting data
506 exclusively from a subgroup of interest were included in the analysis without modification. For
507 studies in which data for these subgroups constituted only part of its dataset, rVLs from the
508 subgroup were collected to calculate the mean, variance and 95% CIs. All calculations were
509 performed in units of $\log_{10}$ copies/ml. In the analysis, we excluded studies with only a single case
510 in our subgroups of interest. Pooled estimates and 95% CIs for each subgroup were calculated
511 using a random-effects meta-analysis, in which between-study heterogeneity was assessed using
512 the I^2 and τ^2 statistics. The weighting for each study in its subgroup was calculated as the
513 reciprocal of the rVL variance.
514
515 **Distribution of rVL**
516 To analyze heterogeneity in rVLs, we pooled the entirety of individual sample data (reported as
517 individual specimen measurements rather through descriptive statistics) in the systematic dataset
518 by disease, COVID-19 subgroups and DFSO. For analyses of SARS-CoV-2 dynamics across
519 DFSO, we included estimated rVLs from negative qRT-PCR measurements of respiratory
520 specimens (n=3, 3, 6, 8, 12, 15, 13, 17 and 14 negative specimens for 2, 3, 4, 5, 6, 7, 8, 9 and 10
521 DFSO, respectively) for cases that had previously been quantitatively confirmed to have
522 COVID-19. These rVLs were estimated based on the reported assay detection limit in the
523 respective study. Probability plots and modified Kolmogorov–Smirnov tests were used to
524 determine the suitability of normal, lognormal, gamma and Weibull distributions to describe the

525 distribution of rVLs for SARS-CoV-2, SARS-CoV-1 and A(H1N1)pdm09. For each virus, the
526 data best conformed to Weibull distributions, which is described by the probability density
527 function

528 $$f(\upsilon) = \frac{\alpha}{\beta}\left(\frac{\upsilon}{\beta}\right)^{\alpha-1} e^{-(\upsilon/\beta)^{\alpha}}, \quad (2)$$

529 where α is the shape factor, β is the scale factor and υ is rVL ($\upsilon \geq 0$ $\log_{10}$ copies/ml). In this
530 distribution, the value of the rVL at the xth percentile was determined using the quantile function,

531 $$\upsilon_x = \beta[-\ln(1-x)]^{1/\alpha}. \quad (3)$$

532 For cp curves, we used eq. (3) to determine rVLs from the 1st cp to the 99th cp (step size, 1%).
533 Curve fitting to eq. (2) and calculation of eq. (3) and its 95% CI was performed using the
534 Distribution Fitter application in Matlab R2019b (MathWorks, Inc., Natick, Massachusetts,
535 USA).
536

537 **Meta-regression of *k* and heterogeneity in rVL**

538 To assess the relationship between *k* and heterogeneity in rVL, we performed a univariate meta-
539 regression ($\log k = a(SD) + b$, where a is the slope for association and b is the intercept)
540 between pooled estimates of *k* (based on studies describing community transmission) for
541 COVID-19 (*k*=0.409)[4-6,105-108], SARS (*k*=0.165)[17] and A(H1N1)pdm09 (*k*=8.155)[22,23] and the SD
542 of the rVLs in each study. Since the negative binomial distribution, from which *k* is derived[17], is
543 analogous to a compound Poisson distribution in which each random variable is Log(k)-
544 distributed, the meta-regression was performed with $\log k$. Based on negligible between-study
545 heterogeneity, we used a fixed-effects model. This analysis assumes that the SD of rVLs in each
546 study estimates SD of rVL for the disease. Thus, for weighting in the meta-regression, we used
547 the proportion of rVL samples for each study relative to the entire systematic dataset ($W_{\text{i}} =$

548 $n_{\mathrm{i}}/n_{\mathrm{total}}$). The regression line, its 95% CI and its Pearson correlation coefficient (r) were
549 presented along with the p-value for association (meta-regression slope t-test for a) between the
550 two variables. The meta-regression assumed that the viability proportion (for viruses exiting the
551 respiratory tract) was similar across cases for a given respiratory infection; it could be a different
552 value for different diseases. The meta-regression also assumed that the rate profile of particles
553 expelled by respiratory activities (e.g., talking) is similar among the diseases. The limit of
554 detection for qRT-PCR instruments used in the included studies did not significantly affect the
555 analysis of heterogeneity in rVL, as these limits tended to be below the values found for
556 specimens with low virus concentrations.
557
558 **Viral kinetics**
559 To model the kinetics of SARS-CoV-2 rVL, we used a mechanistic epithelial cell-limited model
560 for the respiratory tract[109], based on the system of differential equations:

561 $$\frac{dT}{dt} = -\beta TV \tag{4}$$

562 $$\frac{dI}{dt} = \beta TV - \delta I \tag{5}$$

563 $$\frac{dV}{dt} = pI - cV, \tag{6}$$

564 where T is the number of uninfected target cells, I is the number of productively infected cells, V
565 is the rVL, β is the infection rate constant, p is the rate at which airway epithelial cells shed virus
566 to the extracellular fluid, c is the clearance rate of the virus and δ is the clearance rate of
567 productively infected cells. Parameter units are summarized in Extended Data Table 3. Using
568 these parameters, the viral half-life in the respiratory tract ($t_{1/2} = \ln 2/c$) and the half-life of
569 productively infected cells ($t_{1/2} = \ln 2/\delta$) and their 95% CIs could be estimated. Moreover, the

570 cellular basic reproductive number (the expected number of secondary infected cells from a
571 single productively infected cell placed in a population of susceptible cells) was calculated by

572 $$R_{0,c} = \frac{p\beta T_0}{c\delta}, \quad (7)$$

573 where T_0 is the initial number of susceptible cells[109].

574 For initial parameterization, eqs. (4)-(6) were simplified according to a quasi-steady state
575 approximation[110] to

576 $$\frac{dT}{dt} = -\beta TV \quad (8)$$

577 $$\frac{dV}{dt} = rTV - \delta V, \quad (9)$$

578 where $r = p\beta/c$, for a form with greater numerical stability. The system of differential equations
579 was fitted on the mean estimates of SARS-CoV-2 rVL between -2 and 10 DFSO using the
580 entirety of individual sample data in units of copies/ml. Numerical analysis was implemented
581 using the Fit ODE app in OriginPro 2019b (OriginLab Corporation, Northampton,
582 Massachusetts, USA) via the Runge-Kutta method and initial parameters V_0, I_0 and T_0 of 4
583 copies/ml, 0 cells and 5×10^7 cells, respectively, for the range -5 to 10 DFSO. The analysis was
584 first performed with eqs. (8)-(9). These output parameters were then used to initialize final
585 analysis using eqs. (4)-(6), where the estimates for β and δ were input as fixed and variable
586 parameters, respectively. The fitted line and its coefficient of determination (r^2) were presented.

587 To estimate the average incubation period, we extrapolated the kinetic model to 0 and 1
588 $\log_{10}$ copies/ml pre-symptom onset. To estimate the average duration of shedding, we
589 extrapolated the model to 0 $\log_{10}$ copies/ml post-symptom onset. Unlike experimental estimates,
590 this estimate for duration of shedding was not defined by assay detection limits. These analyses
591 had limitations. To estimate the average DFSO on which SARS-CoV-2 concentration reached

592 diagnostic levels, we extrapolated the model pre-symptom onset to the equivalent of 1 and 3
593 $\log_{10}$ copies/ml in specimen concentration (chosen as example assay detection limits), as
594 described by the dilution factor estimation above. The average time from respiratory infection to
595 reach diagnostic levels was then calculated by subtracting these values from the incubation
596 period for 0 $\log_{10}$ copies/ml. However, the extrapolated time for SARS-CoV-2 to reach
597 diagnostic concentrations in the respiratory tract should be validated in tracing studies, in which
598 contacts are prospectively subjected to daily sampling.
599
600 **Considerations for particle dehydration**
601 The desiccation time of a particle in air was described $t_{des} = b^{-1}(d_i^2 - d_{des}^2)$, where b is
602 prefactor for dehydration rate which depends on the environmental conditions, d_i is the initial
603 hydrated diameter and d_{des} is particle diameter after desiccation[111]. After desiccation, the
604 remaining non-volatile matter (ions, molecules, viruses and cells) governs particle size, which is
605 approximately 0.44 times the initial size of particles atomized in the respiratory tract[112].
606 Dehydrated aerodynamic diameter was calculated by $d_a = d_p(\rho/\rho_0)^{1/2}$, where d_p is the
607 dehydrated particle size, ρ is the material density of the respiratory particle and ρ_0 is the
608 reference material density (1 g/cm^3). For conservative estimates, the value of b was taken to be
609 64.9 μm^2/s[113] based on conditions of room temperature and a relative humidity of 59% (near the
610 upper limit of 60% for healthcare and typical indoor specifications)[114]. The equation for
611 desiccation time indicated that respiratory particles begin to dehydrate immediately upon release
612 to the ambient environment. Desiccation occurred rapidly, as the equation estimated that an 11.4-
613 μm particle desiccated to 5 μm in 1.6 s within the model conditions, and this value was an upper
614 limit for the desiccation times of aerosols ($t_{des} \leq 1.6$ s).

615

616 **Likelihood of respiratory particles containing virions**

617 To calculate an unbiased estimator for viral partitioning (the expected number of viable copies in
618 an expelled particle at a given size), we multiplied rVLs with the volume equation for spherical
619 particles during atomization and the estimated viability proportion:

620 $$\lambda = \frac{\pi \rho v_p \gamma \upsilon}{6} d^3, \tag{10}$$

621 where λ is the expectation value, ρ is the material density of the respiratory particle (997 g/m^3),
622 v_p is the volumetric conversion factor (1 ml/g), γ is the viability proportion, υ is the rVL and d is
623 the hydrated diameter of the particle during atomization. The model assumed γ was 0.1% for the
624 viruses. For influenza, approximately 0.1% of copies in particles expelled from the respiratory
625 tract represent viable virus[115], which is equivalent to one in 3 $\log_{10}$ copies/ml for rVL or, after
626 dilution in transport media, roughly one in 4 $\log_{10}$ copies/ml for specimen concentration. Recent
627 reports have detected culture-positive respiratory specimens with SARS-CoV-2 concentrations
628 down to 4 $\log_{10}$ copies/ml[13], including from pediatric patients[62] and in the presymptomatic
629 period[15], suggesting the assumption was also suitable for SARS-CoV-2.

630 Likelihood profiles were determined using Poisson statistics, as described by the probability
631 mass function

632 $$\mathrm{P}(X = k) = \frac{\lambda^k e^{-\lambda}}{k!}, \tag{11}$$

633 where k is the number of virions partitioned within the particle. For λ, 95% CIs were determined
634 using the variance of its rVL estimate. To determine 95% CIs for likelihood profiles from the
635 probability mass function, we used the delta method, which specifies

636 $$\mathrm{Var}\big(g(\boldsymbol{\theta})\big) \approx \sigma^2 \dot{g}(\boldsymbol{\theta})' \mathbf{D} \dot{g}(\boldsymbol{\theta}), \tag{12}$$

637 where $\sigma^2\mathbf{D}$ is the covariance matrix of $\boldsymbol{\theta}$ and $\dot{g}(\boldsymbol{\theta})$ is the gradient of $g(\boldsymbol{\theta})$. For the univariate

638 Poisson distribution, $\sigma^2\mathbf{D} = \lambda$ and

639 $$\dot{g}(\theta) = \frac{\lambda^{k-1}e^{-\lambda}}{k!}(k-\lambda). \quad (13)$$

640 Based on the relative relationship between the residence time of expelled particles before

641 assessment (~5 s)[116] in the referenced study[115] and the estimated dehydration rates of expelled

642 particles, we took the viability proportion (0.1%) to be for dehydrated particles. The model

643 calculated partitioning of copies using the hydrated volume and then applied the viability

644 proportion for number of virions in particles after emission and dehydration. Thus, we compared

645 likelihoods among expelled, dehydrated particles. In Fig. 4, the comparison between hydrated

646 and dehydrated diameters showed only the relationship in particle size and not the relationship in

647 likelihood of containing viable virus. Based on the scope of the study, the model did not account

648 for the virion half-life as particles deposit onto surfaces or remain suspended in air[117].

649

650 **Rate profiles of particles expelled by respiratory activities**

651 For the rate profiles of particles expelled during respiratory activities, we used distributions from

652 the literature. For coughing, we considered the rate (particles/cough) of expelling particles at

653 different sizes, as determined by Loudon and Roberts[118], by calculating the mean number of

654 respiratory particles expelled per cough based on subject tests RI, RII, LI, LII and EI (EII was

655 presumed to be an outlier based on the relative rate when compared to EI). These particles were

656 taken to be dehydrated based on the deposition time in the experiment relative to estimated

657 dehydration rates. We compared this rate profile to that of Duguid[119], which were taken to be

658 hydrated particles based on experimental design. For talking, singing and breathing, we obtained

659 data from Morawaska et al[120]. Rate profiles (particles/min) were calculated by converting the

660 normalized concentration (particles/cm^3) at each particle size based on normalization (32
661 channels per decade) for the aerodynamic particle sizer (APS) used, unit conversion (cm^3 to L)
662 and the sample flow rate (1 L/min). Rate profiles of talking and singing were isolated from
663 breathing by subtracting the contribution of breathing to the combined data. Particles were taken
664 to be dehydrated based on the minimum particle age in the measurements. Based on the APS
665 used, the analyzed range for d_a was 0.3-20 μm. While larger droplets may potentially be expelled
666 by the respiratory activities, the data suggested that their emission rates were minimal, and there
667 was a limited bias associated with instrumentation. We compared these data for talking with rate
668 profiles of talking loudly and talking quietly from Asadi et al[121]. For data reported in a size
669 channel, we took the particle size to be the median value. Curves based on discrete particle
670 measurements were connected using the nonparametric Akima spline function.
671
672 **Shedding virions via respiratory droplets and aerosols**
673 To determine the respiratory shedding rate across particle size, rVL estimates and the hydrated
674 diameters of particles expelled by a respiratory activity were input into eq. (10), and the output
675 was then multiplied by the rate profile of the activity (talking, singing, breathing or coughing).
676 Dehydration and viability considerations were continued from the likelihood models. The model
677 used particle profiles from (coughing) Loudon and Roberts[118] or (talking, singing and breathing)
678 Morawaska et al[120].
679 To determine the total respiratory shedding rate for a given respiratory activity across cp, we
680 determined the cumulative hydrated volumetric rate (by summing the hydrated volumetric rates
681 across particle sizes for that respiratory activity) and input it into eq. (10). Using rVLs as

682 determined by the Weibull quantile functions, we then calculated the Poisson means and their
683 95% CIs at different cps.
684 To assess the relative contribution of aerosols and droplets to mediating respiratory viral
685 shedding for a given respiratory activity, we calculated the proportion of the cumulative hydrated
686 volumetric rate contributed by aerosols ($d_a \leq 5$ μm) or droplets ($d_a > 5$ μm) for that respiratory
687 activity. Since the Poisson mean was proportional to cumulative volumetric rate, this estimate of
688 the relative contribution of aerosols and droplets to respiratory viral shedding was consistent
689 among viruses and cps in the model.
690 In this study, the model for shedding virions via droplets and aerosols did not delineate
691 particles generated in the upper respiratory tract from those generated in the lower respiratory
692 tract, as the sites of atomization remain poorly understood. It also did not differentiate cases with
693 significant expectoration from those without it. In addition, it did not account for individual
694 variation in the profiles of expelled particles; superemitters can expel respiratory particles at
695 rates ~3 times above median[121].
696
697 **Statistical analysis**
698 For data collection, statistical analysis, coding and data visualization, we used Excel v16.40
699 (Microsoft Corporation, Redmond, Washington, USA), OriginPro 2019b (OriginLab
700 Corporation, Northampton, Massachusetts, USA) and Matlab R2019b (MathWorks, Inc., Natick,
701 Massachusetts, USA). Between-study heterogeneity in the random-effects meta-analyses was
702 assessed using the I^2 and τ^2 statistics. Probability plots for normal, lognormal, gamma and
703 Weibull distributions of rVLs were scored based on the Blom method. Modified Kolmogorov-
704 Smirnov tests were used to determine the goodness of fits between rVLs (in $\log_{10}$ copies/ml) and

705 normal, lognormal, gamma or Weibull distributions. By accepting the null hypothesis in the
706 modified Kolmogorov–Smirnov test, the given distribution cannot be rejected to fit the data.
707 Based on fitted Weibull distribution parameters, the Weibull quantile function was used to
708 determine the rVL and its 95% CIs at a given cp. The association between *k* and rVL was
709 assessed via meta-regression, and the *p*-value for association was based on the meta-regression
710 slope *t*-test. Likelihood profiles were determined using the Poisson probability mass function and
711 the unbiased estimator for the expected partitioning of virions at a given particle size. Variance
712 on likelihood estimates was determined via the delta method. Since case variance or sample size
713 may be unequal among the viral infections or subgroups, the two-sided Welch's *t*-test was used
714 to compare the difference of expected rVLs in the meta-analysis and subgroup analyses. For all
715 statistical analyses, the significance level (α) was taken to be 0.05.
716

717 **Data availability**

718 Data will be made available upon request. All raw data, code and model outputs from this study
719 will be made publicly available in online repositories after peer review. Search strategies for the
720 systematic review are shown in Supplementary Tables 1-5. The systematic review protocol was
721 prospectively registered on PROSPERO (registration number, CRD42020204637).
722

723 **References (for Methods)**

724 36 Moher, D., Liberati, A., Tetzlaff, J., Altman, D. G. & Group, P. Preferred reporting items
725 for systematic reviews and meta-analyses: the PRISMA statement. *PLoS Med.* **6**,
726 e1000097, doi:10.1371/journal.pmed.1000097 (2009).

727 37 Higgins, J. P. T. *et al. Cochrane Handbook for Systematic Reviews of Interventions*. (John
728 Wiley & Sons, 2019).
729 38 Munn, Z. *et al.* Methodological quality of case series studies: an introduction to the JBI
730 critical appraisal tool. *JBI Database System Rev Implement Rep*, doi:10.11124/JBISRIR-D-
731 19-00099 (2019).
732 39 Moola, S. *et al.* Chapter 7: Systematic reviews of etiology and risk. *JBI Manual for*
733 *Evidence Synthesis*. (The Joanna Briggs Institute, 2020).
734 40 Munn, Z., Moola, S., Lisy, K., Riitano, D. & Tufanaru, C. Methodological guidance for
735 systematic reviews of observational epidemiological studies reporting prevalence and
736 cumulative incidence data. *Int. J. Evid. Based Healthc.* **13**, 147-153,
737 doi:10.1097/XEB.0000000000000054 (2015).
738 41 Johnston, K. M., Lakzadeh, P., Donato, B. M. K. & Szabo, S. M. Methods of sample size
739 calculation in descriptive retrospective burden of illness studies. *BMC Med. Res. Methodol.*
740 **19**, 9, doi:10.1186/s12874-018-0657-9 (2019).
741 42 Zhang, N. *et al.* Comparative study on virus shedding patterns in nasopharyngeal and fecal
742 specimens of COVID-19 patients. *Sci China Life Sci*, doi:10.1007/s11427-020-1783-9
743 (2020).
744 43 Lavezzo, E. *et al.* Suppression of a SARS-CoV-2 outbreak in the Italian municipality of
745 Vo'. *Nature* **584**, 425-429, doi:10.1038/s41586-020-2488-1 (2020).
746 44 Peng, L. *et al.* SARS-CoV-2 can be detected in urine, blood, anal swabs, and
747 oropharyngeal swabs specimens. *J. Med. Virol.*, doi:10.1002/jmv.25936 (2020).

748 45 To, K. K. *et al.* Temporal profiles of viral load in posterior oropharyngeal saliva samples
749 and serum antibody responses during infection by SARS-CoV-2: an observational cohort
750 study. *Lancet Infect. Dis.* **20**, 565-574, doi:10.1016/S1473-3099(20)30196-1 (2020).
751 46 Zou, L. *et al.* SARS-CoV-2 viral load in upper respiratory specimens of infected patients.
752 *N. Engl. J. Med.* **382**, 1177-1179, doi:10.1056/NEJMc2001737 (2020).
753 47 Fajnzylber, J. M. *et al.* SARS-CoV-2 viral load is associated with increased disease
754 severity and mortality. Preprinted at medRxiv, doi:10.1101/2020.07.15.20131789 (2020).
755 48 Zheng, S. *et al.* Viral load dynamics and disease severity in patients infected with SARS-
756 CoV-2 in Zhejiang province, China, January-March 2020: retrospective cohort study. *BMJ*
757 **369**, m1443, doi:10.1136/bmj.m1443 (2020).
758 49 Lennon, N. J. *et al.* Comparison of viral levels in individuals with or without symptoms at
759 time of COVID-19 testing among 32,480 residents and staff of nursing homes and assisted
760 living facilities in Massachusetts. Preprinted at medRxiv,
761 doi:10.1101/2020.07.20.20157792 (2020).
762 50 Shrestha, N. K. *et al.* Distribution of transmission potential during nonsevere COVID-19
763 illness. *Clin. Infect. Dis.*, doi:10.1093/cid/ciaa886 (2020).
764 51 Shi, F. *et al.* Association of viral load with serum biomakers among COVID-19 cases.
765 *Virology* **546**, 122-126, doi:10.1016/j.virol.2020.04.011 (2020).
766 52 Hung, I. F. *et al.* Triple combination of interferon beta-1b, lopinavir-ritonavir, and ribavirin
767 in the treatment of patients admitted to hospital with COVID-19: an open-label,
768 randomised, phase 2 trial. *Lancet* **395**, 1695-1704, doi:10.1016/S0140-6736(20)31042-4
769 (2020).

770 53 Iwasaki, S. *et al.* Comparison of SARS-CoV-2 detection in nasopharyngeal swab and
771 saliva. *J. Infect.* **81**, e145-e147, doi:10.1016/j.jinf.2020.05.071 (2020).
772 54 Perera, R. A. P. M. *et al.* SARS-CoV-2 virus culture from the upper respiratory tract:
773 Correlation with viral load, subgenomic viral RNA and duration of illness. Preprinted at
774 medRxiv, doi:10.1101/2020.07.08.20148783 (2020).
775 55 Baggio, S. *et al.* SARS-CoV-2 viral load in the upper respiratory tract of children and
776 adults with early acute COVID-19. *Clin. Infect. Dis.*, doi:10.1093/cid/ciaa1157 (2020).
777 56 Lucas, C. *et al.* Longitudinal analyses reveal immunological misfiring in severe COVID-
778 19. *Nature* **584**, 463-469, doi:10.1038/s41586-020-2588-y (2020).
779 57 Argyropoulos, K. V. *et al.* Association of initial viral load in severe acute respiratory
780 syndrome coronavirus 2 (SARS-CoV-2) patients with outcome and symptoms. *Am. J.*
781 *Pathol.* **190**, 1881-1887, doi:10.1016/j.ajpath.2020.07.001 (2020).
782 58 Mitja, O. *et al.* Hydroxychloroquine for early treatment of adults with mild Covid-19: a
783 randomized-controlled trial. *Clin. Infect. Dis.*, doi:10.1093/cid/ciaa1009 (2020).
784 59 Vetter, P. *et al.* Daily viral kinetics and innate and adaptive immune responses assessment
785 in COVID-19: a case series. Preprinted at medRxiv, doi:10.1101/2020.07.02.20143271
786 (2020).
787 60 Xu, Y. *et al.* Characteristics of pediatric SARS-CoV-2 infection and potential evidence for
788 persistent fecal viral shedding. *Nat. Med.* **26**, 502-505, doi:10.1038/s41591-020-0817-4
789 (2020).
790 61 Hurst, J. H. *et al.* SARS-CoV-2 infections among children in the biospecimens from
791 respiratory virus-exposed kids (BRAVE Kids) Study. Preprinted at medRxiv,
792 doi:10.1101/2020.08.18.20166835 (2020).

793 62 L'Huillier, A. G., Torriani, G., Pigny, F., Kaiser, L. & Eckerle, I. Culture-competent
794 SARS-CoV-2 in nasopharynx of symptomatic neonates, children, and adolescents. *Emerg.*
795 *Infect. Dis.* **26**, 2494-2497, doi:10.3201/eid2610.202403 (2020).
796 63 Han, M. S. *et al.* Viral RNA load in mildly symptomatic and asymptomatic children with
797 COVID-19, Seoul, South Korea. *Emerg. Infect. Dis.* **26**, 2497-2499,
798 doi:10.3201/eid2610.202449 (2020).
799 64 Pan, Y., Zhang, D., Yang, P., Poon, L. L. M. & Wang, Q. Viral load of SARS-CoV-2 in
800 clinical samples. *Lancet Infect. Dis.* **20**, 411-412, doi:10.1016/S1473-3099(20)30113-4
801 (2020).
802 65 Han, M. S. *et al.* Sequential analysis of viral load in a neonate and her mother infected with
803 SARS-CoV-2. *Clin. Infect. Dis.*, doi:10.1093/cid/ciaa447 (2020).
804 66 Kawasuji, H. *et al.* Viral load dynamics in transmissible symptomatic patients with
805 COVID-19. Preprinted at medRxiv, doi:10.1101/2020.06.02.20120014 (2020).
806 67 Chu, C. M. *et al.* Initial viral load and the outcomes of SARS. *CMAJ* **171**, 1349-1352,
807 doi:10.1503/cmaj.1040398 (2004).
808 68 Poon, L. L. *et al.* Early diagnosis of SARS coronavirus infection by real time RT-PCR. *J.*
809 *Clin. Virol.* **28**, 233-238, doi:10.1016/j.jcv.2003.08.004 (2003).
810 69 Chen, W. J. *et al.* Nasopharyngeal shedding of severe acute respiratory syndrome-
811 associated coronavirus is associated with genetic polymorphisms. *Clin. Infect. Dis.* **42**,
812 1561-1569, doi:10.1086/503843 (2006).
813 70 Chu, C. M. *et al.* Role of lopinavir/ritonavir in the treatment of SARS: initial virological
814 and clinical findings. *Thorax* **59**, 252-256, doi:10.1136/thorax.2003.012658 (2004).

815 71 Poon, L. L. *et al.* Detection of SARS coronavirus in patients with severe acute respiratory
816 syndrome by conventional and real-time quantitative reverse transcription-PCR assays.
817 *Clin. Chem.* **50**, 67-72, doi:10.1373/clinchem.2003.023663 (2004).
818 72 Chu, C. M. *et al.* Viral load distribution in SARS outbreak. *Emerg. Infect. Dis.* **11**, 1882-
819 1886, doi:10.3201/eid1112.040949 (2005).
820 73 Hung, I. F. *et al.* Viral loads in clinical specimens and SARS manifestations. *Emerg. Infect.*
821 *Dis.* **10**, 1550-1557, doi:10.3201/eid1009.040058 (2004).
822 74 Cheng, V. C. *et al.* Viral replication in the nasopharynx is associated with diarrhea in
823 patients with severe acute respiratory syndrome. *Clin. Infect. Dis.* **38**, 467-475,
824 doi:10.1086/382681 (2004).
825 75 Peiris, J. S. *et al.* Clinical progression and viral load in a community outbreak of
826 coronavirus-associated SARS pneumonia: a prospective study. *Lancet* **361**, 1767-1772,
827 doi:10.1016/s0140-6736(03)13412-5 (2003).
828 76 Loeb, M. *et al.* Longitudinal study of influenza molecular viral shedding in Hutterite
829 communities. *J. Infect. Dis.* **206**, 1078-1084, doi:10.1093/infdis/jis450 (2012).
830 77 Suess, T. *et al.* Shedding and transmission of novel influenza virus A/H1N1 infection in
831 households--Germany, 2009. *Am. J. Epidemiol.* **171**, 1157-1164, doi:10.1093/aje/kwq071
832 (2010).
833 78 Li, C. C. *et al.* Correlation of pandemic (H1N1) 2009 viral load with disease severity and
834 prolonged viral shedding in children. *Emerg. Infect. Dis.* **16**, 1265-1272,
835 doi:10.3201/eid1608.091918 (2010).

836 79 Lu, P. X. *et al.* Relationship between respiratory viral load and lung lesion severity: a study
837 in 24 cases of pandemic H1N1 2009 influenza A pneumonia. *J. Thorac. Dis.* **4**, 377-383,
838 doi:10.3978/j.issn.2072-1439.2012.08.02 (2012).
839 80 Ip, D. K. M. *et al.* The dynamic relationship between clinical symptomatology and viral
840 shedding in naturally acquired seasonal and pandemic influenza virus infections. *Clin.*
841 *Infect. Dis.* **62**, 431-437, doi:10.1093/cid/civ909 (2016).
842 81 Rath, B. *et al.* Virus load kinetics and resistance development during oseltamivir treatment
843 in infants and children infected with Influenza A(H1N1) 2009 and Influenza B viruses.
844 *Pediatr. Infect. Dis. J.* **31**, 899-905, doi:10.1097/INF.0b013e31825c7304 (2012).
845 82 Meschi, S. *et al.* Duration of viral shedding in hospitalized patients infected with pandemic
846 H1N1. *BMC Infect. Dis.* **11**, 140, doi:10.1186/1471-2334-11-140 (2011).
847 83 Wu, U. I., Wang, J. T., Chen, Y. C. & Chang, S. C. Severity of pandemic H1N1 2009
848 influenza virus infection may not be directly correlated with initial viral load in upper
849 respiratory tract. *Influenza Other Respir. Viruses* **6**, 367-373, doi:10.1111/j.1750-
850 2659.2011.00300.x (2012).
851 84 Yang, J. R., Lo, J., Ho, Y. L., Wu, H. S. & Liu, M. T. Pandemic H1N1 and seasonal H3N2
852 influenza infection in the human population show different distributions of viral loads,
853 which substantially affect the performance of rapid influenza tests. *Virus Res.* **155**, 163-
854 167, doi:10.1016/j.virusres.2010.09.015 (2011).
855 85 Launes, C. *et al.* Viral load at diagnosis and influenza A H1N1 (2009) disease severity in
856 children. *Influenza Other Respir. Viruses* **6**, e89-92, doi:10.1111/j.1750-
857 2659.2012.00383.x (2012).

858 86 Killingley, B. *et al.* Virus shedding and environmental deposition of novel A (H1N1)
859 pandemic influenza virus: interim findings. *Health Technol. Assess.* **14**, 237-354,
860 doi:10.3310/hta14460-04 (2010).
861 87 Lee, N. *et al.* Viral clearance and inflammatory response patterns in adults hospitalized for
862 pandemic 2009 influenza A(H1N1) virus pneumonia. *Antivir. Ther.* **16**, 237-247,
863 doi:10.3851/IMP1722 (2011).
864 88 Chan, P. K. *et al.* Clinical and virological course of infection with haemagglutinin D222G
865 mutant strain of 2009 pandemic influenza A (H1N1) virus. *J. Clin. Virol.* **50**, 320-324,
866 doi:10.1016/j.jcv.2011.01.013 (2011).
867 89 Hung, I. F. *et al.* Effect of clinical and virological parameters on the level of neutralizing
868 antibody against pandemic influenza A virus H1N1 2009. *Clin. Infect. Dis.* **51**, 274-279,
869 doi:10.1086/653940 (2010).
870 90 To, K. K. *et al.* Delayed clearance of viral load and marked cytokine activation in severe
871 cases of pandemic H1N1 2009 influenza virus infection. *Clin. Infect. Dis.* **50**, 850-859,
872 doi:10.1086/650581 (2010).
873 91 Thai, P. Q. *et al.* Pandemic H1N1 virus transmission and shedding dynamics in index case
874 households of a prospective Vietnamese cohort. *J. Infect.* **68**, 581-590,
875 doi:10.1016/j.jinf.2014.01.008 (2014).
876 92 Ito, M. *et al.* Detection of pandemic influenza A (H1N1) 2009 virus RNA by real-time
877 reverse transcription polymerase chain reaction. *Pediatr. Int.* **54**, 959-962,
878 doi:10.1111/j.1442-200X.2012.03720.x (2012).

879 93 Li, I. W. *et al.* The natural viral load profile of patients with pandemic 2009 influenza
880 A(H1N1) and the effect of oseltamivir treatment. *Chest* **137**, 759-768,
881 doi:10.1378/chest.09-3072 (2010).
882 94 Esposito, S. *et al.* Viral shedding in children infected by pandemic A/H1N1/2009 influenza
883 virus. *Virol J.* **8**, 349, doi:10.1186/1743-422X-8-349 (2011).
884 95 Lee, C. K. *et al.* Comparison of pandemic (H1N1) 2009 and seasonal influenza viral loads,
885 Singapore. *Emerg. Infect. Dis.* **17**, 287-291, doi:10.3201/eid1702.100282 (2011).
886 96 Cowling, B. J. *et al.* Comparative epidemiology of pandemic and seasonal influenza A in
887 households. *N. Engl. J. Med.* **362**, 2175-2184, doi:10.1056/NEJMoa0911530 (2010).
888 97 To, K. K. *et al.* Viral load in patients infected with pandemic H1N1 2009 influenza A
889 virus. *J. Med. Virol.* **82**, 1-7, doi:10.1002/jmv.21664 (2010).
890 98 Alves, V. R. G. *et al.* Influenza A(H1N1)pdm09 infection and viral load analysis in
891 patients with different clinical presentations. *Mem. Inst. Oswaldo Cruz* **115**, e200009,
892 doi:10.1590/0074-02760200009 (2020).
893 99 Cheng, P. K. *et al.* Performance of laboratory diagnostics for the detection of influenza
894 A(H1N1)v virus as correlated with the time after symptom onset and viral load. *J. Clin.*
895 *Virol.* **47**, 182-185, doi:10.1016/j.jcv.2009.11.022 (2010).
896 100 Ngaosuwankul, N. *et al.* Influenza A viral loads in respiratory samples collected from
897 patients infected with pandemic H1N1, seasonal H1N1 and H3N2 viruses. *Virol J.* **7**, 75,
898 doi:10.1186/1743-422X-7-75 (2010).
899 101 Duchamp, M. B. *et al.* Pandemic A(H1N1)2009 influenza virus detection by real time RT-
900 PCR: is viral quantification useful? *Clin. Microbiol. Infect.* **16**, 317-321,
901 doi:10.1111/j.1469-0691.2010.03169.x (2010).

902 102 Watanabe, M., Nukuzuma, S., Ito, M. & Ihara, T. Viral load and rapid diagnostic test in
903 patients with pandemic H1N1 2009. *Pediatr. Int.* **53**, 1097-1099, doi:10.1111/j.1442-
904 200X.2011.03489.x (2011).
905 103 Warnke, P., Warning, L. & Podbielski, A. Some are more equal - a comparative study on
906 swab uptake and release of bacterial suspensions. *PLoS One* **9**, e102215,
907 doi:10.1371/journal.pone.0102215 (2014).
908 104 Wan, X., Wang, W., Liu, J. & Tong, T. Estimating the sample mean and standard deviation
909 from the sample size, median, range and/or interquartile range. *BMC Med. Res. Methodol.*
910 **14**, 135, doi:10.1186/1471-2288-14-135 (2014).
911 105 Adam, D. C. *et al.* Clustering and superspreading potential of SARS-CoV-2 infections in
912 Hong Kong. *Nat. Med.*, doi:10.1038/s41591-020-1092-0 (2020).
913 106 Riou, J. & Althaus, C. L. Pattern of early human-to-human transmission of Wuhan 2019
914 novel coronavirus (2019-nCoV), December 2019 to January 2020. *Euro Surveill.* **25**,
915 doi:10.2807/1560-7917.ES.2020.25.4.2000058 (2020).
916 107 Zhang, Y., Li, Y., Wang, L., Li, M. & Zhou, X. Evaluating transmission heterogeneity and
917 super-spreading event of COVID-19 in a metropolis of China. *Int. J. Environ. Res. Public*
918 *Health* **17**, doi:10.3390/ijerph17103705 (2020).
919 108 Tariq, A. *et al.* Real-time monitoring the transmission potential of COVID-19 in
920 Singapore, March 2020. *BMC Med.* **18**, 166, doi:10.1186/s12916-020-01615-9 (2020).
921 109 Baccam, P., Beauchemin, C., Macken, C. A., Hayden, F. G. & Perelson, A. S. Kinetics of
922 influenza A virus infection in humans. *J. Virol.* **80**, 7590-7599, doi:10.1128/JVI.01623-05
923 (2006).

924 110 Ikeda, H. *et al.* Quantifying the effect of Vpu on the promotion of HIV-1 replication in the
925 humanized mouse model. *Retrovirology* **13**, 23, doi:10.1186/s12977-016-0252-2 (2016).
926 111 Wells, W. F. On air-borne infection: study II. droplets and droplet nuclei. *Am. J.*
927 *Epidemiol.* **20**, 611-618, doi:10.1093/oxfordjournals.aje.a118097 (1934).
928 112 Nicas, M., Nazaroff, W. W. & Hubbard, A. Toward understanding the risk of secondary
929 airborne infection: emission of respirable pathogens. *J. Occup. Environ. Hyg.* **2**, 143-154,
930 doi:10.1080/15459620590918466 (2005).
931 113 Stadnytskyi, V., Bax, C. E., Bax, A. & Anfinrud, P. The airborne lifetime of small speech
932 droplets and their potential importance in SARS-CoV-2 transmission. *Proc. Natl. Acad.*
933 *Sci. U. S. A.* **117**, 11875-11877, doi:10.1073/pnas.2006874117 (2020).
934 114 Institute, T. F. G. *Guidelines for design and construction of health care facilities*. (The
935 American Institute of Architects, 2006).
936 115 Yan, J. *et al.* Infectious virus in exhaled breath of symptomatic seasonal influenza cases
937 from a college community. *Proc. Natl. Acad. Sci. U. S. A.* **115**, 1081-1086,
938 doi:10.1073/pnas.1716561115 (2018).
939 116 McDevitt, J. J. *et al.* Development and performance evaluation of an exhaled-breath
940 bioaerosol collector for influenza virus. *Aerosol Sci. Technol.* **47**, 444-451,
941 doi:10.1080/02786826.2012.762973 (2013).
942 117 van Doremalen, N. *et al.* Aerosol and surface stability of SARS-CoV-2 as compared with
943 SARS-CoV-1. *N. Engl. J. Med.* **382**, 1564-1567, doi:10.1056/NEJMc2004973 (2020).
944 118 Loudon, R. G. & Roberts, R. M. Droplet expulsion from the respiratory tract. *Am. Rev.*
945 *Respir. Dis.* **95**, 435-442, doi:10.1164/arrd.1967.95.3.435 (1967).

946 119 Duguid, J. P. The size and the duration of air-carriage of respiratory droplets and droplet-
947 nuclei. *J. Hyg. (Lond.)* **44**, 471-479, doi:10.1017/s0022172400019288 (1946).
948 120 Morawska, L. *et al.* Size distribution and sites of origin of droplets expelled from the
949 human respiratory tract during expiratory activities. *J. Aerosol Sci* **40**, 256-269,
950 doi:10.1016/j.jaerosci.2008.11.002 (2009).
951 121 Asadi, S. *et al.* Aerosol emission and superemission during human speech increase with
952 voice loudness. *Sci. Rep.* **9**, 2348, doi:10.1038/s41598-019-38808-z (2019).
953

954 **Acknowledgements**

955 We thank T. Alba (Toronto) for discussion on statistical methods. We thank E. Lavezzo and A.
956 Chrisanti (Padova) for responses to data inquiries. This work was supported by the Natural
957 Sciences and Engineering Research Council of Canada (NSERC) and the Toronto COVID-19
958 Action Fund. P.Z.C. was supported by the NSERC Vanier Scholarship (608544). D.N.F. was
959 supported by the Canadian Institutes of Health Research (Canadian COVID-19 Rapid Research
960 Fund, OV4-170360). F.X.G. was supported by the NSERC Senior Industrial Research Chair.
961

962 **Author contributions**

963 P.Z.C. designed the study, performed analyses, interpreted results and drafted the manuscript.
964 P.Z.C. and N.B. conducted screening, appraised studies and drafted the review protocol. Z.P.
965 developed and conducted the systematic review search. M.K. and D.N.F. assessed methods,
966 interpreted results and contributed to the discussion. All authors reviewed and revised the
967 manuscript. F.X.G. secured funds, interpreted results and supervised the project.
968

969 **Competing interests** The authors declare no competing interests.

970

971 **Supplementary information** is available for this paper.

972

973 **Correspondence and requests for materials** should be addressed to F.X.G.

Subgroup, study ref.	Cases No.	Cases Type	Specimens No.	Specimens DFSO	Specimens Type	Respiratory viral load, log_{10} copies/ml (95% CI)	*p*-value for difference
SARS-CoV-2							
42	4	H, A, S	9	4 to 10	NPS, OPS	4.12 (3.18-5.05)	
43	102	H, C, A, P, S, Ps, As	109	-2 to 10	NPS, OPS	4.63 (4.34-4.92)	
44	6	H, A, S	6	3 to 8	OPS	5.13 (4.83-5.42)	
45	23	H, A, S	51	0 to 10	ETA, POS	5.29 (4.65-5.93)	
46	14	H, A, S, As	55	0 to 10	NPS, OPS	5.30 (4.87-5.74)	
47	-	H, N, A, S	31	2 to 10	NPS, OPS, Spu	5.41 (4.81-6.01)	
61	133	C, A, P, S, Ps, As	133	-3 to 10	NPS	5.59 (5.31-5.88)	
48	-	H, A, S	19	1 to 10	POS, Spu	5.62 (5.22-6.03)	
60	7	H, P, S, Ps, As	14	-1 to 10	NPS	5.69 (5.26-6.12)	
64	75	H, S, Ps	104	-1 to 8	OPS, Spu	5.98 (5.31-6.66)	
49	2,200	C, A, P, As	2,200	0	NPS	6.01 (5.93-6.09)	
50	171	N, A, S	171	0 to 10	NPS	6.07 (5.79-6.34)	
51	103	H, N, A, S	103	0 to 8	NPS, OPS	6.10 (5.98-6.23)	
13	9	H, A, S, As	133	2 to 10	NPS, OPS, Spu	6.21 (5.90-6.52)	
52	41	H, A, S	310	2 to 10	NPS, OPS, POS	6.28 (6.05-6.50)	
53	5	H, A, S	5	7 to 9	NPS	6.48 (5.26-7.70)	
54	-	H, A, S, As	38	0 to 9	NPA, NPS, OPS, Spu	6.52 (5.77-7.27)	
66	16	H, A, P, S, Ps, As	17	-1 to 10	NPS	6.77 (5.96-7.58)	
55	405	H, A, P, S	405	0 to 5	NPS	6.95 (6.78-7.17)	
62	23	H, P, S	23	0 to 4	NPS	7.20 (6.23-8.16)	
56	24	H, A, S	33	0 to 10	NPS	7.51 (6.97-8.05)	
57	205	H, N, A, S	205	0 to 10	NPS	7.55 (7.30-7.81)	
35	-	H, A, S	154	0 to 10	NPS, Spu	7.83 (7.58-8.08)	
65	2	H, A, P, S	8	4 to 10	NPS, OPS	7.91 (6.69-9.12)	
58	148	N, A, S	296	1 to 8	NPS	8.04 (7.81-8.28)	
63	12	H, P, S, As	27	0 to 10	NPS	8.07 (7.47-8.67)	
59	5	H, A, S	63	0 to 10	NPS, OPS	8.34 (7.95-8.73)	
Overall (Q_{26} = 13.2, p = 0.98, I^2 = 0.0%)						6.21 (6.10-6.31)	-
SARS-CoV-1							
67	133	H, A, S	133	1 to 7	NPA	2.89 (2.24-3.55)	
68	40	H, A, S	40	1 to 3	NPA	4.18 (3.24-5.12)	
69	153	H, A, S	153	0 to 19	NPS	4.90 (4.64-5.16)	
70	11	H, A, S	11	20	NPS	5.09 (3.60-6.59)	
71	-	H, A, S	43	1 to 10	NPA	5.62 (4.94-6.30)	
72	57	H, A, S	57	0 to 6	NPA	5.86 (5.36-6.35)	
73	60	H, A, S	60	10 to 15	NPA	6.65 (6.21-7.08)	
74	59	H, A, S	59	10	NPA	6.67 (6.23-7.11)	
75	14	H, A, S	42	5 to 15	NPA	6.73 (6.28-7.18)	
Overall (Q_8 = 2.16, p = 0.98, I^2 = 0.0%)						5.85 (5.42-6.28)	0.148
Influenza A(H1N1)pdm09							
76	97	C, A, P, S, Ps, As	218	-2 to 9	NPS	5.10 (4.93-5.27)	
77	51	C, A, P, S, As	129	1 to 7	NPA, NPS, OPS	5.17 (4.85-5.49)	
78	581	H, A, P, S	581	1 to 8	OPS	5.46 (5.38-5.55)	
79	13	H, A, P, S	25	2 to 9	NPS	5.69 (4.97-6.41)	
80	17	C, A, P, S	20	0 to 6	NPS, OPS	5.73 (5.17-6.29)	
81	27	H, P, S	41	2 to 7	NPS	5.84 (5.41-6.27)	
82	533	H, A, S	533	0 to 9	NPS	6.09 (5.98-6.20)	
83	64	H, N, A, P, S	89	1 to 7	NPS	6.18 (5.79-6.58)	
84	633	H, N, A, P, S	533	0 to 3	OPS	6.31 (6.07-6.56)	
85	47	H, P, S	47	1 to 4	NPA	6.49 (6.01-6.98)	
86	12	H, C, A, P, S	21	3 to 5	NPS	6.83 (6.16-7.51)	
87	48	H, A, S	48	0 to 7	NPA	6.84 (6.44-7.23)	
88	58	H, A, S	58	0 to 9	NPA, NPS, OPS	6.86 (6.52-7.20)	
89	87	H, N, A, P, S	87	0 to 7	NPA, NPS	6.87 (6.60-7.15)	
90	50	H, A, S	50	0 to 9	NPA, NPS	7.04 (6.51-7.58)	
91	33	C, A, P, S, Ps, As	123	-1 to 8	NPS, OPS	7.16 (6.95-7.37)	
92	34	H, A, P, S	34	0 to 2	NPS	7.18 (6.77-7.59)	
93	27	H, A, P, S	59	0 to 7	NPA, NPS, OPS	7.21 (6.83-7.58)	
94	74	H, P, S	282	1 to 9	NPS	7.22 (6.99-7.44)	
95	578	H, A, P, S	578	1 to 7	NPS	7.22 (7.11-7.34)	
96	45	N, C, A, P, S	54	0 to 8	NPS, OPS	7.28 (6.85-7.71)	
97	22	H, A, P, S	22	0 to 7	NPA, NPS, OPS	7.29 (6.53-8.05)	
98	86	N, C, A, P, S, As	86	0 to 8	NPA, NPS, OPS	7.32 (6.94-7.71)	
99	60	H, A, P, S	60	0 to 3	NPA	7.38 (6.98-7.78)	
100	12	H, A, P, S	33	2 to 9	NPA, NPS, OPS	7.39 (6.81-7.97)	
101	209	H, C, P, S	209	0 to 7	NPS	8.21 (8.06-8.36)	
102	251	H, P, S	251	0 to 2	NPA	8.42 (8.28-8.56)	
Overall (Q_{26} = 9.53, p > 0.99, I^2 = 0.0%)						6.72 (6.61-6.83)	<0.0001

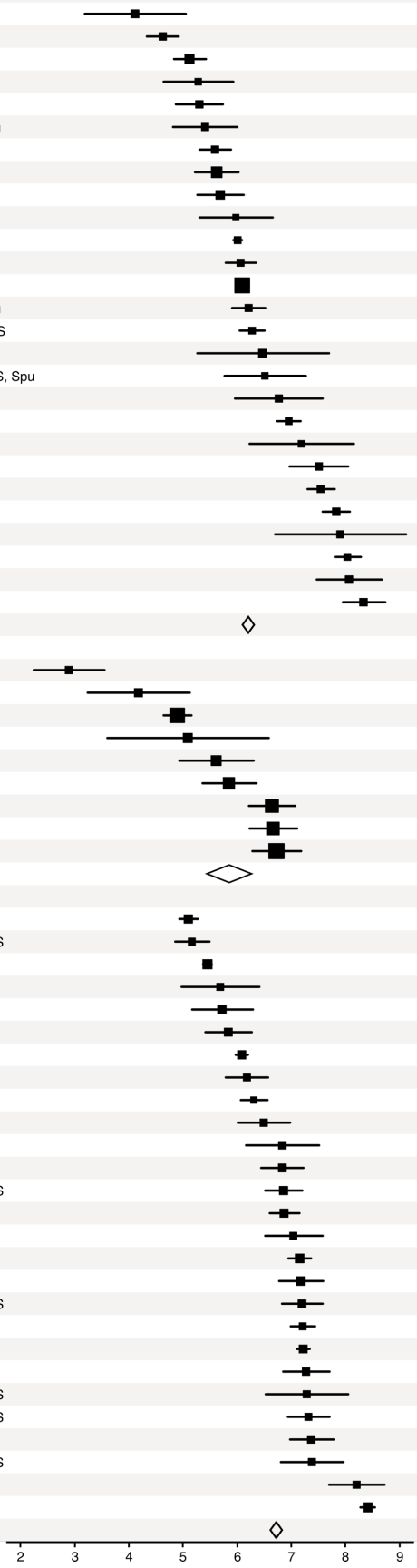

974

975 **Extended Data Fig. 1. Meta-analysis of respiratory viral loads of SARS-CoV-2, SARS-CoV-**
976 **1 and influenza A(H1N1)pdm09 during the infectious period.** Random-effects meta-analyses
977 comparing the expected rVLs for COVID-19, SARS and A(H1N1)pdm09 cases during the
978 infectious period. Quantitative specimen measurements were used to estimate rVLs, which refer
979 to virus concentrations in the respiratory tract. Case types: hospitalized (H), not admitted (N),
980 community (C), adult (A), pediatric (P), symptomatic (S), presymptomatic (Ps) and
981 asymptomatic (As). Specimen types: endotracheal aspirate (ETA), nasopharyngeal aspirate
982 (NPA), nasopharyngeal swab (NPS), oropharyngeal swab (OPS), posterior oropharyngeal saliva
983 (POS) and sputum (Spu). Studies after ref. 35 are listed in Methods. Dashes denote case numbers
984 that were not obtained. Box sizes are proportional to weighting in the overall estimates. Two-
985 sided Welch's *t*-test (relative to SARS-CoV-2), non-significance (p>0.05).

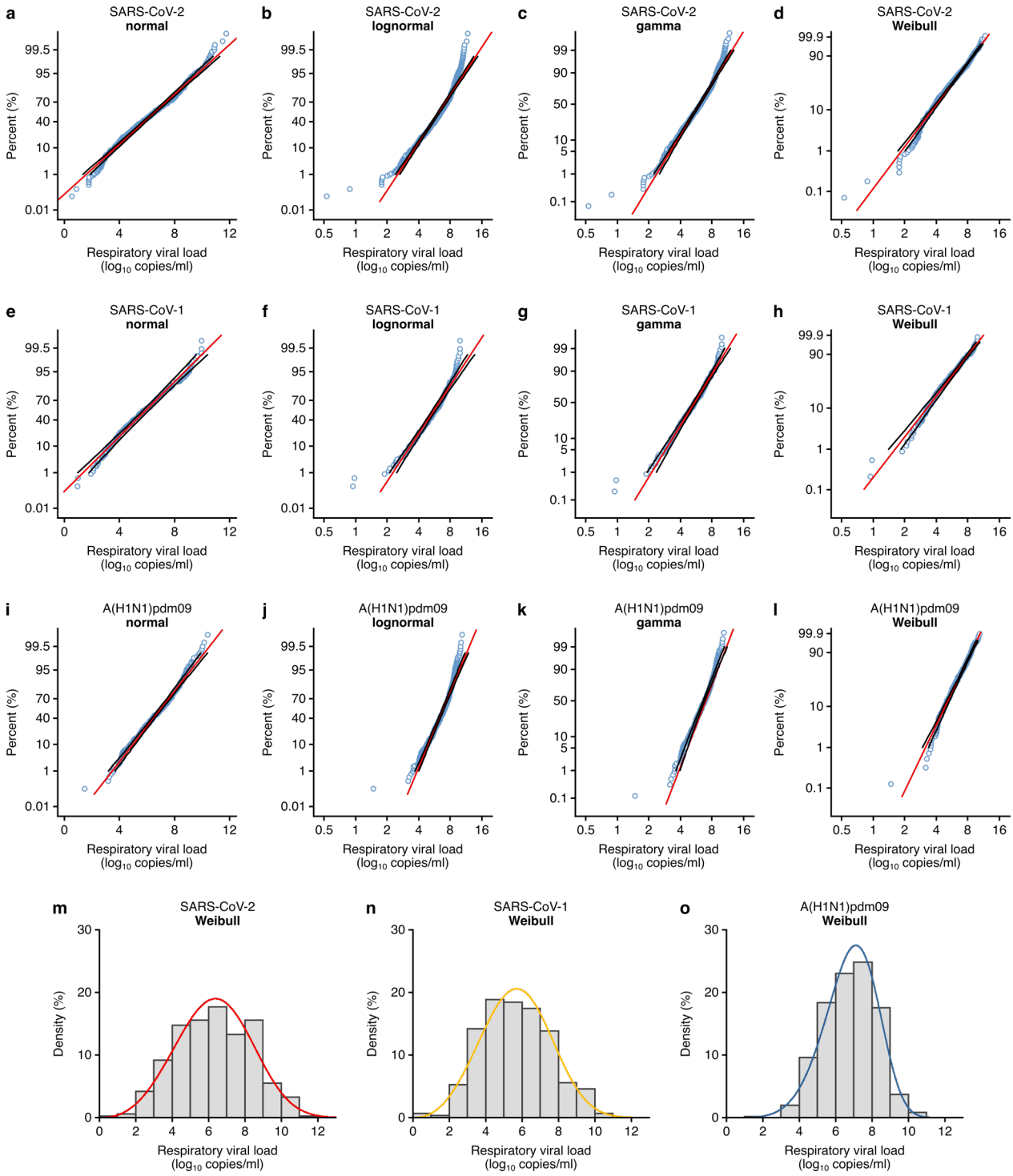

986

987 **Extended Data Fig. 2. Respiratory viral loads for SARS-CoV-2, SARS-CoV-1 and**

988 **A(H1N1)pdm09 best conform to Weibull distributions. a-d**, Normal ($p \leq 0.01$) (**a**), lognormal

989 ($p \leq 0.01$) (**b**), gamma ($p \leq 0.005$) (**c**) and Weibull ($p > 0.10$, not significant [NS]) (**d**) probability

990 plots for individual sample data of SARS-CoV-2 rVLs across DFSO in the systematic dataset
991 (n=916 samples from n=19 studies). **e-h**, Normal (p>0.10, NS) (**e**), lognormal (p≤0.01) (**f**),
992 gamma (p>0.05, NS) (**g**) and Weibull (p>0.10, NS) (**h**) probability plots for individual sample
993 data of SARS-CoV-1 rVLs in the systematic dataset (n=303 samples from n=5 studies). **i-l**,
994 Normal (p≤0.01) (**i**), lognormal (p≤0.01) (**j**), gamma (p≤0.005) (**k**) and Weibull (p>0.10, NS) (**l**)
995 probability plots for individual sample data of A(H1N1)pdm09 rVLs in the systematic dataset
996 (n=512 samples from n=10 studies). These categories included only rVL data from positive
997 (above the detection limit) qRT-PCR measurements. The p-values were determined using the
998 modified Kolmogorov-Smirnov test for the goodness of fit of the distributions. When the null
999 hypothesis is accepted (NS at p>0.05), the probability density function cannot be rejected to
1000 describe the distribution of the data. Blue circles, black lines and red lines represent individual
1001 sample data, expected distributions and 95% CIs, respectively. **m-o**, Histograms and fitted
1002 Weibull distributions of the above data for SARS-CoV-2 (**m**), SARS-CoV-1 (**n**) and
1003 A(H1N1)pdm09 (**o**).

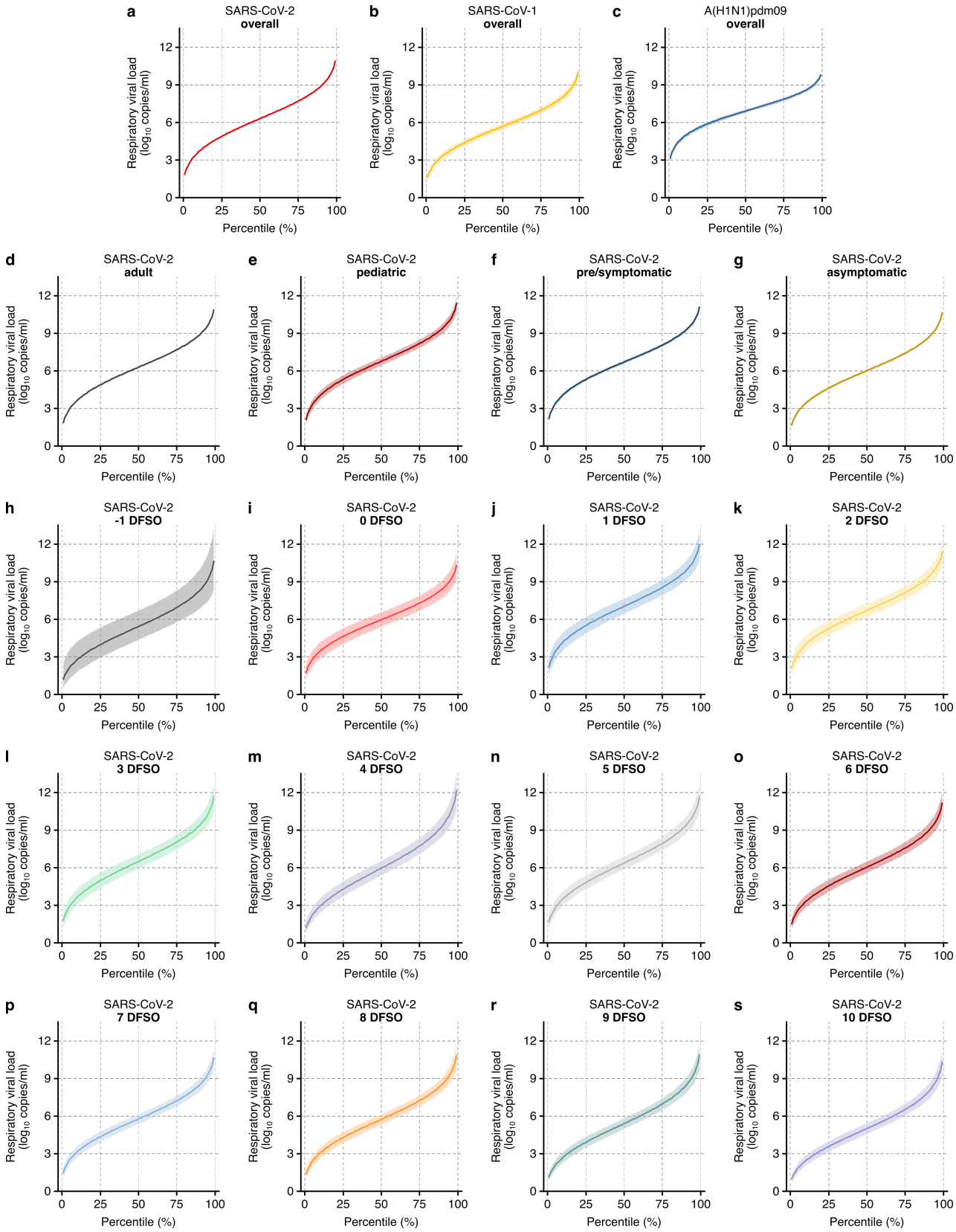
a
SARS-CoV-2
overall
b
SARS-CoV-1
overall
c
A(H1N1)pdm09
overall
d
SARS-CoV-2
adult
e
SARS-CoV-2
pediatric
f
SARS-CoV-2
pre/symptomatic
g
SARS-CoV-2
asymptomatic
h
SARS-CoV-2
-1 DFSO
i
SARS-CoV-2
0 DFSO
j
SARS-CoV-2
1 DFSO
k
SARS-CoV-2
2 DFSO
l
SARS-CoV-2
3 DFSO
m
SARS-CoV-2
4 DFSO
n
SARS-CoV-2
5 DFSO
o
SARS-CoV-2
6 DFSO
p
SARS-CoV-2
7 DFSO
q
SARS-CoV-2
8 DFSO
r
SARS-CoV-2
9 DFSO
s
SARS-CoV-2
10 DFSO
Respiratory viral load
(log10 copies/ml)
Percentile (%)
0
3
6
9
12
0
25
50
75
100

1004

1005 **Extended Data Fig. 3. Respiratory viral loads across case percentiles for viruses, subgroups**
1006 **and days from symptom onset. a, b**, Estimated rVLs of SARS-CoV-2 (**a**), SARS-CoV-1 (**b**)
1007 and A(H1N1)pdm09 (**c**) across cp during the infectious periods. **d-g**, Estimated SARS-CoV-2
1008 rVLs across cp for adult (**d**), pediatric (**e**), symptomatic/presymptomatic (**f**) and asymptomatic
1009 (**g**) cases during the infectious period. **h-s**, Estimated SARS-CoV-2 rVLs across cp on different
1010 days of the infectious period. Earlier presymptomatic days were excluded based on limited data.
1011 Data ranged between the 1st and 99th cps. Sample numbers, distribution parameters and
1012 descriptive statistics are summarized in Extended Data Table 2. Lines and bands represent
1013 estimates and 95% CIs, respectively.

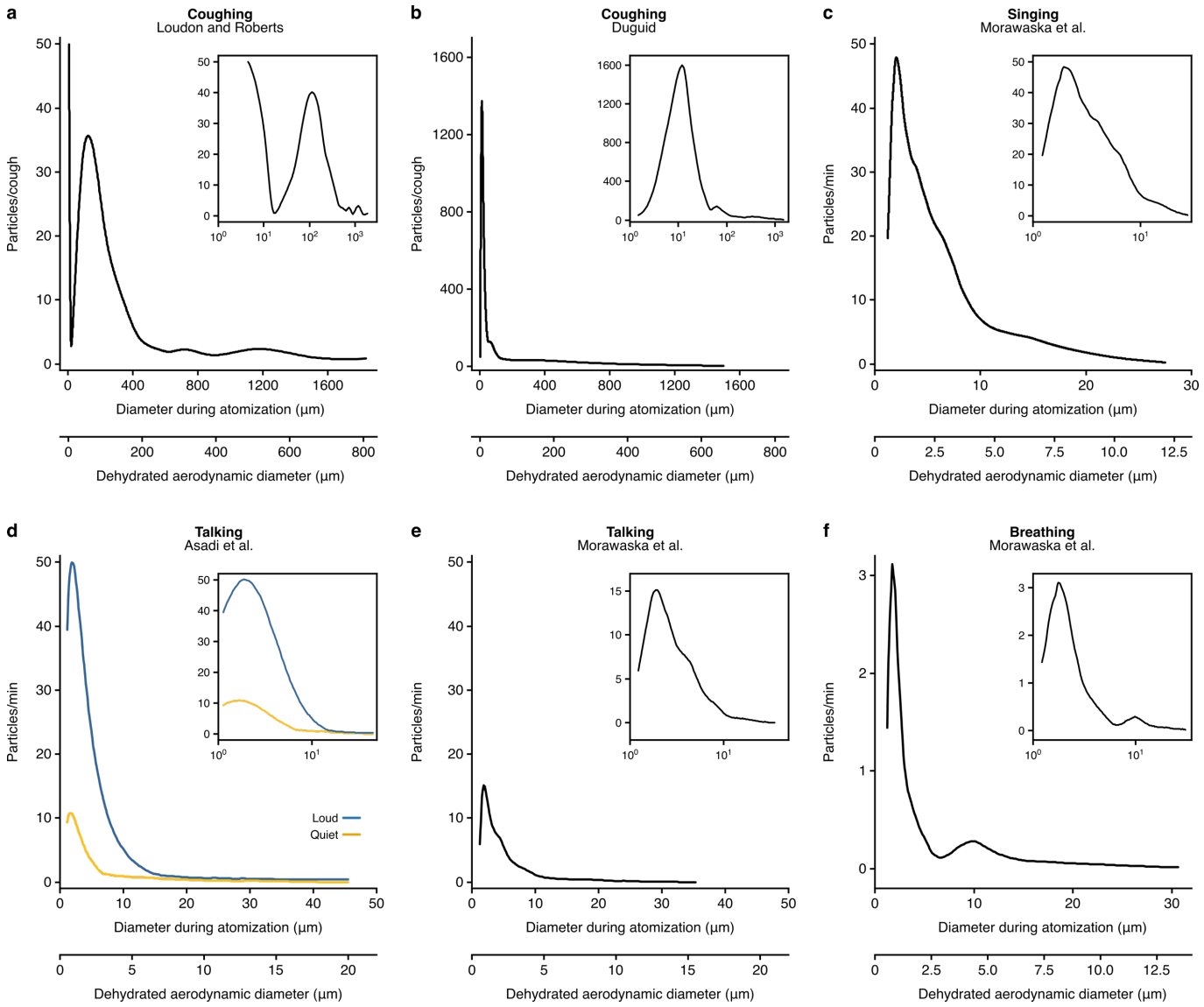

Extended Data Fig. 4. Rate profiles for particle expelled by respiratory activities. a,b, Rate profiles of particles expelled during coughing. The data were obtained from Loudon and Roberts[118] (**a**) and Duguid[119] (**b**). **c**, Rate profile of particles expelled during singing, as obtained from Morawaska et al[120]. **d,e**, Rate profiles of particles expelled during talking. The data were obtained from Asadi et al[121] (**d**) and Morawaska et al[120]. (**e**). **f**, Rate profiles of particles expelled during breathing at a natural pace, as obtained from Morawaska et al[120]. Insets, particle profiles with a logarithmic axis for diameter during atomization.

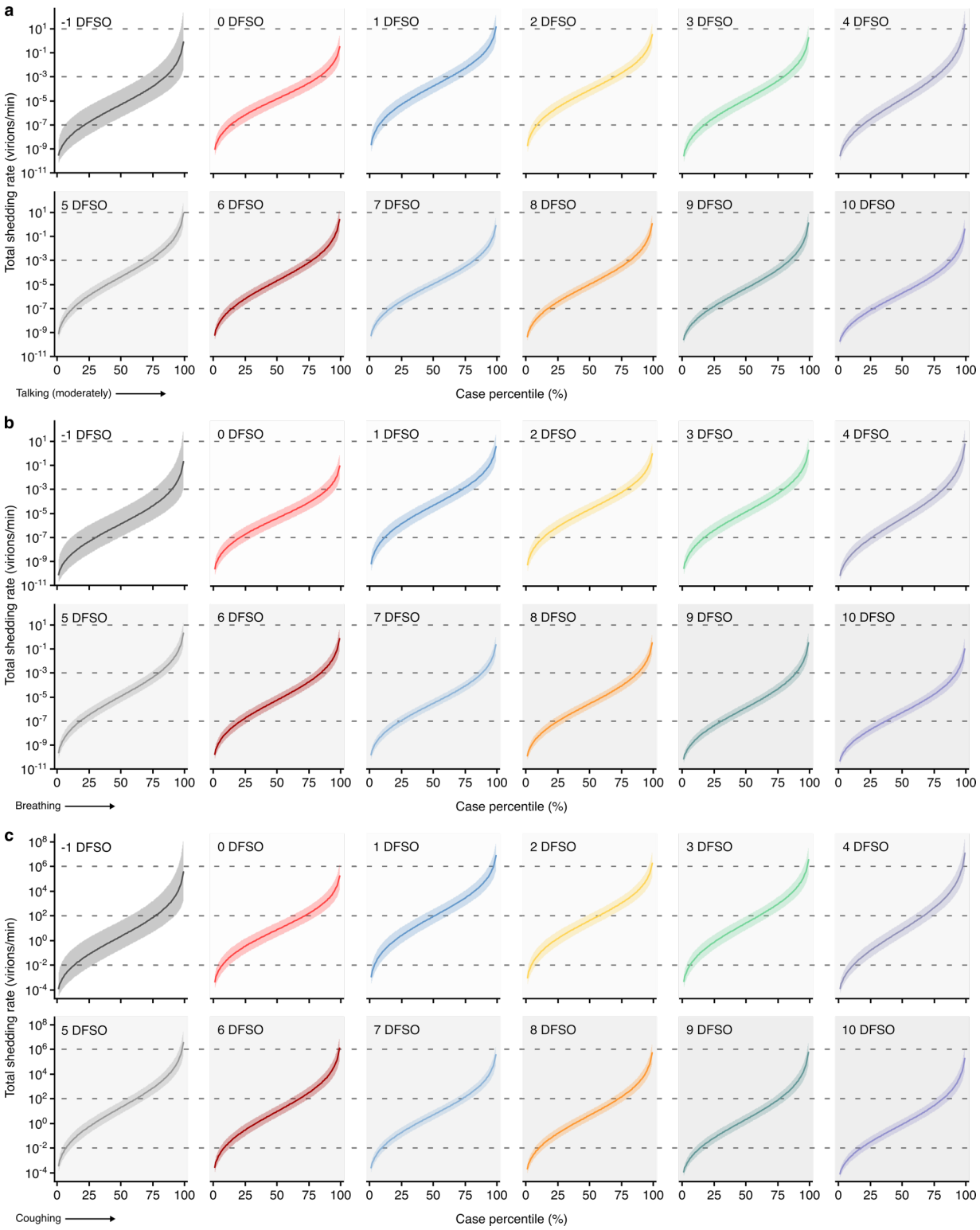

Extended Data Fig. 5. Heterogeneity in shedding SAR-CoV-2 via talking, breathing and coughing. a-c, Case heterogeneity in the total SARS-CoV-2 shedding rate (over all particle

1025 sizes) by talking at a moderate level (**a**), breathing (**b**) or coughing (**c**) for COVID-19 cases

1026 across the infectious period. Earlier presymptomatic days were excluded based on limited data.

1027 Data represent estimated rates for viable virus and range between the 1st and 99th cps. Lines and

1028 bands represent estimates and 95% CIs, respectively.

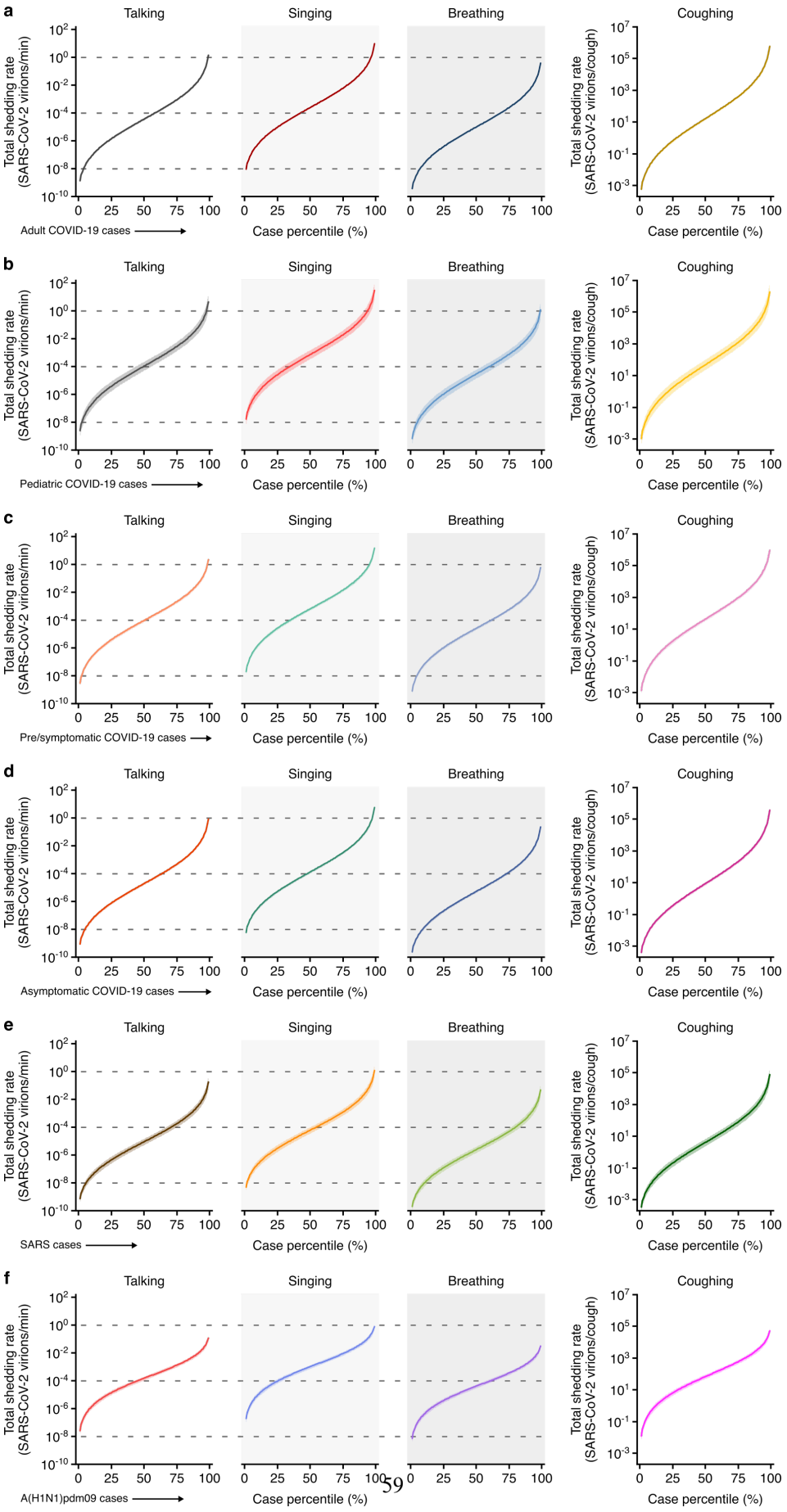
a
Talking
Singing
Breathing
Coughing
Total shedding rate (SARS-CoV-2 virions/min)
Total shedding rate (SARS-CoV-2 virions/cough)
Adult COVID-19 cases
Case percentile (%)
b
Pediatric COVID-19 cases
c
Pre/symptomatic COVID-19 cases
d
Asymptomatic COVID-19 cases
e
SARS cases
f
A(H1N1)pdm09 cases

1029

1030 **Extended Data Fig. 6. Heterogeneity in respiratory virus shedding for subgroup COVID-**
1031 **19, SARS and A(H1N1)pdm09 cases. a-d**, Case heterogeneity in the total SARS-CoV-2
1032 shedding rate for adult (**a**), pediatric (**b**), symptomatic/presymptomatic (**c**) and asymptomatic (**d**)
1033 COVID-19 cases via talking, singing, breathing and coughing during the infectious period. **e,f**,
1034 Case heterogeneity in the total SARS-CoV-1 (**e**) and A(H1N1)pdm09 (**f**) shedding rates via
1035 talking, singing, breathing and coughing for SARS and A(H1N1)pdm09 cases, respectively,
1036 during the infectious periods. Data represent estimated rates for viable virus and range between
1037 the 1st and 99th cps. Lines and bands represent estimates and 95% CIs, respectively.
1038

1039 **Extended Data Table 1 I Characteristics of included studies**

Study*	Country	No. of cases included (no. of specimens)	No. of pediatric cases (no. of specimens)	No. of asymptomatic cases (no. of specimens)	Disease caused by virus	Case definition (WHO)	Pharmaco-therapy (type)†	Individual data extracted (diluent volume reported)‡	Adjusted viral load§ (type of specimen)	Weight, % (meta-analysis category)‖	Weight, % (meta-regression)	Risk of bias¶
Argyropoulos et al. (2020)[57]	USA	205 (205)	0	0	COVID-19	Confirmed	No	No (no)	Yes (NPS)	2.3 (V), 2.9 (A), 2.5 (S/Ps)	2.12	********
Baggio et al. (2020)[55]	Switzerland	405 (405)	58 (58)	0	COVID-19	Confirmed	No	Yes (no)	Yes (NPS)	2.1 (V), 2.7 (A), 11.5 (P), 2.2 (S/Ps)	4.18	*******
Fajnzylber et al. (2020)[47]	USA	- (31)	0	0	COVID-19	Confirmed	No	Yes (yes)	Yes (NPS, OPS) No (Spu)	2.8 (V), 3.5 (A), 3.0 (S/Ps)	0.32	********
Han et al. (2020)[65]	South Korea	2 (8)	1 (6)	0	COVID-19	Confirmed	No	Yes (no)	Yes (NPS, OPS)	2.7 (V), 2.8 (S/Ps)	0.08	******
Han et al. (2020)[63]	South Korea	12 (27)	12 (27)	3 (7)	COVID-19	Confirmed	No	Yes (no)	Yes (NPS)	3.2 (V), 18.5 (P), 3.2 (S/Ps), 31.0 (As)	0.28	********
Hung et al. (2020)[52]	China	41 (310)	0	0	COVID-19	Confirmed	No (control group)	No (no)	Yes (NPS, OPS, POS)	2.0 (V), 2.4 (A), 2.1 (S)	3.20	********
Hurst et al. (2020)[61]	USA	133 (133)	54 (54)	52 (52)	COVID-19	Confirmed	No	Yes (no)	Yes (NPS)	2.8 (V), 15.3 (P), 3.0 (S/Ps), 24.1 (As)	1.37	********
Iwasaki et al. (2020)[53]	Japan	5 (5)	0	0	COVID-19	Confirmed	No	Yes (no)	Yes (NPS)	4.2 (V), 5.2 (A), 4.5 (S/Ps)	0.05	***
Kawasuji et al. (2020)[66]	Japan	16 (16)	-	-	COVID-19	Confirmed	Yes (antivirals - type not reported)	Yes (no)	Yes (NPS)	2.8 (V)	0.18	*****
L'Huillier et al. (2020)[62]	Switzerland	23 (23)	23 (23)	0	COVID-19	Confirmed	No	Yes (no)	Yes (NPS)	1.5 (V), 8.4 (P), 1.6 (S/Ps)	0.24	********
Lavezzo et al. (2020)[43]	Italy	103 (110)	2 (3)	49 (49)	COVID-19	Confirmed	No	Yes (yes)	Yes (NPS, OPS)	3.2 (V), 4.0 (A), 14.4 (P), 3.3 (S/Ps), 27.9 (A)	1.13	*******
Lennon et al. (2020)[49]	USA	2,200 (2,200)	18 (18)	2,200 (2,200#)	COVID-19	Confirmed	No	No (yes)	Yes (NPS)	2.0 (V), 2.5 (A), 17.0 (As)	22.70	********
Lucas et al. (2020)[56]	USA	24 (33)	0	0	COVID-19	Confirmed	Moderate and severe patients (tocilizumab)	Yes (yes)	Yes (NPS)	3.3 (V), 4.0 (A), 3.5 (S/Ps)	0.34	*******
Mitja et al. (2020)[58]	Spain	148 (296)	0	0	COVID-19	Confirmed	No (control group)	No (no)	Yes (NPS)	1.9 (V), 2.3 (A), 2.0 (S/Ps)	3.05	********
Pan et al. (2020)[64]	China	75 (104)	-	0	COVID-19	Confirmed	No	Yes (no)	Yes (OPS) No (Spu)	0.7 (V), 0.7 (S/Ps)	1.07	****

Peng et al. (2020)[44]	China	6 (6)	0	0	COVID-19	Confirmed	Yes (arbidol, lopinavir, ritonavir)	Yes (no)	Yes (OPS)	6.6 (V), 8.2 (A), 7.1 (S/Ps)	0.06	********
Perera et al. (2020)[54]	China	- (36)	0	-	COVID-19	Confirmed	No	Yes (no)	Yes (NPA, NPS, OPS, Spu)	1.5 (V), 1.8 (A)	0.39	****
Shi et al. (2020)[51]	China	103 (103)	0	0	COVID-19	Confirmed	No	Yes (no)	Yes (NPS, OPS)	19.0 (V), 23.4 (A), 20.2 (S/Ps)	1.06	*****
Shrestha et al. (2020)[50]	USA	171 (171)	0	0	COVID-19	Confirmed	No	Yes (no)	Yes (NPS)	2.4 (V), 3.0 (A), 2.6 (S/Ps)	1.76	*******
To et al. (2020)[45]	China	23 (51)	0	0	COVID-19	Confirmed	No	Yes (yes)	Yes (ETA, POS)	1.5 (V), 1.8 (A), 1.6 (S/Ps)	0.53	*********
van Kampen et al. (2020)[35]	The Netherlands	- (154)	0	0	COVID-19	Confirmed	No	Yes (yes)	Yes (NPS, Spu)	3.2 (V), 4.0 (A), 3.5 (S/Ps)	1.59	*******
Vetter et al. (2020)[59]	Switzerland	5 (63)	0	0	COVID-19	Confirmed	No	Yes (yes)	Yes (NPS, OPS)	3.3 (V), 4.1 (A), 3.5 (S/Ps)	0.65	*********
Wölfel et al. (2020)[13]	Germany	9 (136)	0	1 (4)	COVID-19	Confirmed	No	Yes (yes)	Yes (NPS, OPS) No (Spu)	2.5 (V), 3.0 (A), 3.2 (S)	1.37	*******
Xu et al. (2020)[60]	China	7 (14)	7 (14)	1 (1)	COVID-19	Confirmed	No	Yes (no)	Yes (NPS)	5.5 (V), 31.8 (P), 5.8 (S/Ps),	0.14	********
Zhang et al. (2020)[42]	China	9 (9)	0	0	COVID-19	Confirmed	No	Yes (no)	Yes (NPS, OPS)	4.0 (V), 5.0 (A), 4.3 (S/Ps)	0.09	********
Zheng et al. (2020)[48]	China	- (19)	0	0	COVID-19	Confirmed	No	Yes (no)	Yes (POS, Spu)	10.0 (V), 12.4 (A), 10.7 (S/Ps)	0.20	*******
Zou et al. (2020)[46]	China	14 (55)	0	1 (4)	COVID-19	Confirmed	No	Yes (no)	Yes (NPS, OPS)	3.0 (V), 3.7 (A), 3.1 (S/Ps)	0.57	********
Chen et al. (2006)[69]	China	154 (154#)	0	0	SARS	Confirmed	Yes (oseltamivir, broad-spectrum antibiotics, ribavirin)	Yes (no)	Yes (NPS)	17.9 (V)	1.58	********
Chu et al. (2004)[67]	China	133 (133)	0	0	SARS	Confirmed	No	No (yes)	Yes (NPA)	2.9 (V)	1.37	*********
Chu et al. (2004)[70] ☆	China	11 (11)	0	0	SARS	Confirmed	No (control group)	Yes (yes)	Yes (NPS)	6.7 (V)	0.11	*********
Chu et al. (2005)[72]	China	57 (57)	0	0	SARS	Confirmed	No	Yes (yes)	Yes (NPA)	11.6 (V)	0.59	*********
Cheng et al. (2004)[74]	China	59 (59)	0	0	SARS	Confirmed	Yes (ribavirin, hydrocortisone, prednisolone, methylpredni-solone)	Yes (yes)	Yes (NPA)	14.2 (V)	0.61	********
Hung et al. (2004)[73]	China	60 (60)	0	0	SARS	Confirmed	Yes (ribavirin, hydrocortisone, prednisolone,	No (yes)	Yes (NPA)	14.7 (V)	0.62	*******

							methylpredni-solone)					
Peiris et al. (2003)[75] ☆	China	14 (42)	0	0	SARS	Confirmed	Yes (ribavirin, hydrocortisone, prednisolone, methylpredni-solone)	Yes (no)	Yes (NPA)	19.2 (V)	0.43	********
Poon et al. (2003)[68]	China	40 (40)	0	0	SARS	Confirmed	No	No (yes)	Yes (NPA)	4.6 (V)	0.41	*****
Poon et al. (2004)[71]	China	- (43)	0	0	SARS	Confirmed	-	No (yes)	Yes (NPA)	8.2 (V)	0.44	*****
Alves et al. (2020)[98]	Brazil	86 (86)	-	15 (15)	Influenza A(H1N1)pdm09	Confirmed	No	No (yes)	Yes (NPA, NPS, OPS)	2.4 (V)	0.89	*****
Chan et al. (2011)[88]	China	58 (58)	0	0	Influenza A(H1N1)pdm09	Confirmed	No (pretreatment)	Yes (no)	Yes (NPA, NPS, OPS)	4.6 (V)	0.60	******
Cheng et al. (2010)[99]	China	60 (60)	-	0	Influenza A(H1N1)pdm09	Confirmed	No (pretreatment)	No (no)	Yes (NPA)	3.3 (V)	0.62	******
Cowling et al. (2010)[96]	China	45 (54)	22 (31)	0	Influenza A(H1N1)pdm09	Confirmed	Yes (22 cases on oseltamivir)	Yes (yes)	Yes (NPS, OPS)	3.1 (V)	0.56	*******
Duchamp et al. (2010)[101]	France	209 (209)	209 (209)	0	Influenza A(H1N1)pdm09	Confirmed	Yes (oseltamivir, zanamivir)	No (yes)	Yes (NPS)	2.4 (V)	2.16	*****
Esposito et al. (2011)[94]	Italy	74 (282)	74 (282)	0	Influenza A(H1N1)pdm09	Confirmed	No	Yes (yes)	Yes (NPS)	2.2 (V)	2.91	******
Hung et al. (2010)[89]	China	87 (87)	-	0	Influenza A(H1N1)pdm09	Confirmed	Yes (oseltamivir)	Yes (no)	Yes (NPA, NPS)	4.7 (V)	0.90	******
Ip et al. (2016)[80]	China	17 (20)	7 (-)	0	Influenza A(H1N1)pdm09	Confirmed	No	Yes (no)	Yes (NPS, OPS)	5.0 (V)	0.21	******
Ito et al. (2012)[92]	Japan	34 (34)	-	0	Influenza A(H1N1)pdm09	Confirmed	No (pretreatment)	Yes (yes)	Yes (NPS)	5.5 (V)	0.35	*****
Killingley et al. (2010)[86]	United Kingdom	12 (21)	-	0	Influenza A(H1N1)pdm09	Confirmed	Yes (oseltamivir)	Yes (yes)	Yes (NPS)	3.3 (V)	0.22	********
Launes et al. (2012)[85]	Spain	47 (47)	47 (47)	0	Influenza A(H1N1)pdm09	Confirmed	No (pretreatment)	No (no)	Yes (NPA)	3.0 (V)	0.48	*******
Lee et al. (2011)[87]	China	48 (48)	0	0	Influenza A(H1N1)pdm09	Confirmed	No (pretreatment)	No (no)	Yes (NPA)	4.1 (V)	0.50	******
Lee et al. (2011)[95]	Singapore	578 (578)	231 (231)	0	Influenza A(H1N1)pdm09	Confirmed	No (pretreatment)	No (no)	Yes (NPS)	4.1 (V)	5.96	*********
Li et al. (2010)[78]	China	581 (581)	522 (522)	0	Influenza A(H1N1)pdm09	Confirmed	No (pretreatment)	No (no)	Yes (OPS)	6.7 (V)	5.99	******
Li et al. (2010)[93]	China	27 (59)	-	0	Influenza A(H1N1)pdm09	Confirmed	No (non-treated group)	No (no)	Yes (NPA, NPS, OPS)	3.8 (V)	0.61	*******
Loeb et al. (2012)[76]	Canada	97 (218)	-	- (17)	Influenza A(H1N1)pdm09	Confirmed	No	No (no)	Yes (NPS)	4.9 (V)	2.25	*******

Lu et al. (2012)[79]	China	13 (25)	-	0	Influenza A(H1N1)pdm09	Confirmed	Yes (oseltamivir, zanamivir)	Yes (no)	Yes (NPS)	2.4 (V)	0.26	*******
Meschi et al. (2011)[82]	Italy	533 (533)	0	0	Influenza A(H1N1)pdm09	Confirmed	No (pretreatment)	No (no)	Yes (NPS)	4.8 (V)	5.50	*********
Ngaosuwankul et al. (2010)[100]	China	12 (33)	-	0	Influenza A(H1N1)pdm09	Confirmed	No (pretreatment)	No (yes)	Yes (NPA, NPS, OPS)	2.8 (V)	0.34	******
Rath et al. (2012)[81]	Germany	27 (41)	27 (41)	0	Influenza A(H1N1)pdm09	Confirmed	Yes (oseltamivir)	Yes (yes)	Yes (NPS)	4.1 (V)	0.42	*********
Suess et al. (2010)[77]	Germany	51 (129)	12 (-)	1 (1)	Influenza A(H1N1)pdm09	Confirmed	Yes (oseltamivir)	No (no)	Yes (NPA, NPS, OPS)	2.4 (V)	1.33	******
Thai et al. (2014)[91]	Vietnam	33 (123)	16 (-)	5 (28)	Influenza A(H1N1)pdm09	Confirmed	Yes (oseltamivir)	Yes (yes)	Yes (NPS)	5.8 (V)	1.27	*******
To et al. (2010)[90]	China	50 (50)	0	0	Influenza A(H1N1)pdm09	Confirmed	Yes (oseltamivir, nebulized zanamivir)	No (no)	Yes (NPA, NPS)	2.2 (V)	0.52	******
To et al. (2010)[97]	China	22 (22)	-	0	Influenza A(H1N1)pdm09	Confirmed	No (pretreatment)	No (no)	Yes (NPA, NPS, OPS)	2.5 (V)	0.23	*****
Watanabe et al. (2011)[102]	Japan	251 (251)	251 (251)	0	Influenza A(H1N1)pdm09	Confirmed	No (pretreatment)	No (yes)	Yes (NPA)	6.6 (V)	2.59	**********
Wu et al. (2012)[83]	China	64 (89)	-	0	Influenza A(H1N1)pdm09	Confirmed	Yes (oseltamivir)	No (yes)	Yes (NPS)	2.3 (V)	0.92	******
Yang et al. (2011)[84]	China	251 (251)	-	0	Influenza A(H1N1)pdm09	Confirmed	N/A	No (yes)	Yes (OPS)	0.8 (V)	6.53	******

*References 13 and 35 are listed in the main body while those 42 and after are listed in Methods. Data shown as "-" were not obtained from the paper or authors.
†Responses of "no" for pharmacotherapy are based on no pharmacotherapy given to any patients or none reported in the study.
‡For studies reporting specimen measurements as individual sample data (either in numerical or graphical formats), the sample data was extracted for analysis.
§Specimen measurements were converted to rVLs based on the dilution factor for specimens immersed in transport media.
‖Abbreviations: viral meta-analysis (V), adult subgroup (A), pediatric subgroup (P), symptomatic/presymptomatic subgroup (S/Ps), asymptomatic subgroup (As).
¶The hybrid JBI Critical Appraisal Checklist was used, with more stars indicating lower risk of bias. Results from each study are shown in Supplementary Table 6.
#For these studies, only 2,147 (Lennon et al.) and 134 (Chen et al.) individual specimen measurements were obtained for the individual sample datasets.
☆For Chu et al., only specimen measurements at 20 DFSO were extracted, as 5-15 DFSO were equivalent specimens as those reported in Peiris et al.

1048 **Extended Data Table 2 | Descriptive parameters for subgroups of respiratory viral loads based on individual sample data**

			Weibull distribution parameters		Respiratory viral load, log_{10} copies/ml				
Category	***n*** * **(specimens)**	***n*** * **(studies)**	**Scale factor (95% CI)**	**Shape factor (95% CI)**	**Mean (95% CI)**†	**SD**†	**90th percentile (95% CI)**‡	**95th percentile (95% CI)**‡	**99th percentile (95% CI)**‡
SARS-CoV-2 (overall)§	3,778	24	7.01 (6.94-7.07)	3.47 (3.38-3.56)	6.28 (6.22-6.35)	2.04	8.91 (8.82-9.00)	9.61 (9.51-9.71)	10.88 (10.75-11.02)
SARS-CoV-1 (overall)§	303	5	6.34 (6.12-6.56)	3.37 (3.09-3.68)	5.69 (5.48-5.90)	1.86	8.11 (7.83-8.40)	8.77 (8.45-9.11)	9.96 (9.54-10.41)
A(H1N1)pdm09 (overall)§	512	10	7.39 (7.27-7.51)	5.43 (5.07-5.81)	6.81 (6.69-6.94)	1.45	8.62 (8.47-8.76)	9.04 (8.88-9.21)	9.79 (9.59-10.00)
SARS-CoV-2 (adult)§	3,532	18	6.99 (6.92-7.06)	3.47 (3.38-3.56)	6.27 (6.20-6.34)	2.04	8.89 (8.80-8.98)	9.59 (9.49-9.70)	10.86 (10.72-11.00)
SARS-CoV-2 (pediatric)§	185	7	7.47 (7.17-7.79)	3.65 (3.26-4.08)	6.73 (6.43-7.02)	2.06	9.39 (9.01-9.79)	10.09 (9.65-10.56)	11.36 (10.78-11.97)
SARS-CoV-2 (symptomatic/presymptomatic)§	1,503	20	7.39 (7.28-7.49)	3.79 (3.64-3.94)	6.66 (6.56-6.76)	2.01	9.21 (9.08-9.34)	9.87 (9.72-10.02)	11.06 (10.86-11.26)
SARS-CoV-2 (asymptomatic)§	2,212	6	6.72 (6.63-6.81)	3.32 (3.22-3.44)	6.01 (5.93-6.09)	2.02	8.64 (8.52-8.75)	9.35 (9.21-9.48)	10.64 (10.46-10.81)
SARS-CoV-2 (all DFSO)§	916	19	7.04 (6.90-7.18)	3.47 (3.30-3.65)	6.32 (6.19-6.45)	2.04	8.95 (8.78-9.13)	9.66 (9.45-9.86)	10.93 (10.66-11.21)
SARS-CoV-2 (-3 DFSO)‖	1	1	-	-	10.34	-	-	-	-
SARS-CoV-2 (-2 DFSO)‖	3	2	-	-	4.22 (2.41-6.02)	1.59	-	-	-
SARS-CoV-2 (-1 DFSO)	15	5	6.17 (5.11-7.47)	2.82 (1.89-4.19)	5.48 (4.25-6.70)	2.21	8.30 (6.88-10.02)	9.11 (7.44-11.16)	10.62 (8.38-13.45)
SARS-CoV-2 (0 DFSO)	48	10	6.63 (6.08-7.23)	3.46 (2.81-4.26)	5.97 (5.43-6.51)	1.85	8.43 (7.75-9.18)	9.10 (8.32-9.96)	10.31 (9.29-11.43)
SARS-CoV-2 (1 DFSO)	59	10	7.79 (7.23-8.40)	3.58 (2.91-4.40)	7.00 (6.42-7.59)	2.26	9.83 (9.12-10.61)	10.58 (9.75-11.49)	11.93 (10.84-13.14)
SARS-CoV-2 (2 DFSO)¶	69	13	7.42 (6.93-7.95)	3.61 (2.97-4.39)	6.67 (6.15-7.19)	2.17	9.35 (8.72-10.03)	10.06 (9.32-10.85)	11.33 (10.35-12.40)
SARS-CoV-2 (3 DFSO)¶	71	15	7.27 (6.74-7.84)	3.25 (2.69-3.93)	6.50 (5.96-7.04)	2.29	9.39 (8.71-10.14)	10.19 (9.38-11.06)	11.63 (10.54-12.82)
SARS-CoV-2 (4 DFSO)¶	81	15	6.84 (6.27-7.45)	2.66 (2.22-3.17)	6.08 (5.52-6.63)	2.51	9.36 (8.58-10.21)	10.34 (9.40-11.36)	12.15 (10.87-13.59)
SARS-CoV-2 (5 DFSO)¶	87	14	7.16 (6.67-7.68)	3.14 (2.65-3.72)	6.40 (5.91-6.89)	2.29	9.33 (8.69-10.02)	10.15 (9.40-10.96)	11.64 (10.63-12.74)
SARS-CoV-2 (6 DFSO)¶	102	14	6.81 (6.37-7.27)	3.09 (2.63-3.62)	6.07 (5.63-6.51)	2.24	8.92 (8.34-9.53)	9.71 (9.03-10.44)	11.16 (10.24-12.17)
SARS-CoV-2 (7 DFSO)¶	125	18	6.50 (6.13-6.89)	3.10 (2.69-3.58)	5.82 (5.45-6.19)	2.10	8.50 (8.01-9.03)	9.26 (8.67-9.88)	10.63 (9.84-11.49)
SARS-CoV-2 (8 DFSO)¶	119	18	6.49 (6.09-6.91)	2.99 (2.59-3.46)	5.79 (5.40-6.18)	2.14	8.57 (8.04-9.13)	9.35 (8.73-10.02)	10.80 (9.96-11.71)
SARS-CoV-2 (9 DFSO)¶	117	18	6.18 (5.76-6.63)	2.72 (2.35-3.15)	5.51 (5.11-5.91)	2.20	8.40 (7.82-9.01)	9.25 (8.57-9.98)	10.83 (9.90-11.85)
SARS-CoV-2 (10 DFSO)¶	110	16	5.76 (5.34-6.20)	2.61 (2.25-3.03)	5.13 (4.73-5.53)	2.11	7.92 (7.34-8.55)	8.76 (8.07-9.51)	10.33 (9.38-11.37)

1049 *These two columns summarize the cumulative number of specimens (left) collected from the number of studies (right) for each category in the systematic dataset.
1050 †The mean and sample SD were calculated on the entire set of individual sample data for each category.
1051 ‡The Weibull quantile distributions were used to determine rVLs at the 90th, 95th and 99th cps.
1052 §These categories included only rVL data from positive (above the detection limit) qRT-PCR measurements.
1053 ‖Data for earlier DFSO were excluded from distribution fitting based on limited data, and empty cells were marked with "-".
1054 ¶These categories included negative qRT-PCR measurements (set at the detection limit to estimate rVLs; *n* = 3, 3, 6, 8, 12, 15, 13, 17 and 14 specimens for 2-10 DFSO, respectively) for cases that tested
1055 positive at an earlier DFSO.

1056 **Extended Data Table 3 | Model parameters describing SARS-CoV-2 kinetics in the respiratory tract**

Parameter	Description	Value (95% CI)	Units
β	Infection rate constant	4.02 (3.01-5.03)	$\times 10^{-7}$ (copies/ml)$^{-1}$ day^{-1}
p	Cellular shedding rate of virus	1.11 (0.51-1.71)	copies/ml day^{-1} cell^{-1}
c	Clearance rate of virus	3.82 (0.17-7.47)	day^{-1}
δ	Clearance rate of infected epithelial cells	0.55 (0.23-0.87)	day^{-1}
$R_{0,c}$	Cellular basic reproductive number	10.6	unitless
V_0*	Initial rVL parameter	4	copies/ml
I_0*	Initial number of infected cells	0	cells
T_0*	Initial number of uninfected cells	5×10^7	cells

1057 *Initial values were used as inputs for the numerical estimation of the model parameters.